

PAPER • OPEN ACCESS

# Update on the status of the IFMIF-DONES test systems

To cite this article: S. Becerril *et al* 2025 *Nucl. Fusion* **65** 122010

View the [article online](#) for updates and enhancements.

You may also like

- [Analysis of the linear and nonlinear stability of Alfvén eigenmodes and fish-bones in JET DT discharges: mode identification and shear flows generation](#)  
J. Varela, J. García, S. Mazzi et al.
- [Metrics and extrapolation of resonant magnetic perturbation thresholds for ELM suppression](#)  
N.C. Logan, S.K. Kim, S.M. Yang et al.
- [Low collisionality, peeling limited pedestals in JET-ILW: effect of density and isotope mass on pedestal structure, pedestal stability and pedestal prediction in deuterium and mixed deuterium/tritium plasmas](#)  
L. Frassinetti, D. King, S. Saarelma et al.

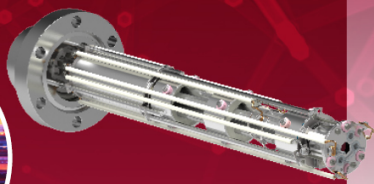
Mass spectrometers for vacuum, gas, plasma and surface science

**HIDEN**  
ANALYTICAL

## Ultra-high Resolution Mass Spectrometers for the Study of Hydrogen Isotopes and Applications in Nuclear Fusion Research

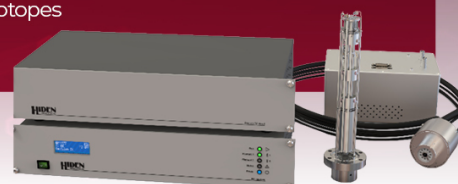
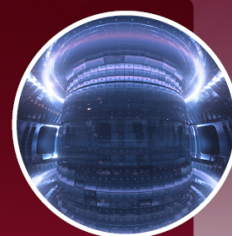
### DLS Series

- **Unique** Dual Mass range / Zone H functionality
- For the measurement of overlapping species
- He/D2, CH2D2/H2O, Ne/D2O



### HAL 101X

- Monitoring, diagnostics and analysis applications in tokamak and torus operations
- Unique design avoids all radiation shielding requirements
- Featuring TIMS mode for real-time quantification of hydrogen and helium isotopes



[www.HidenAnalytical.com](http://www.HidenAnalytical.com)



[info@hiden.co.uk](mailto:info@hiden.co.uk)

# Update on the status of the IFMIF-DONES test systems

S. Becerril<sup>1,\*</sup>, J. Castellanos<sup>2</sup>, P. Araya<sup>1</sup>, F. Arranz<sup>3</sup>, C. Caballero<sup>1</sup>, T. Dézsi<sup>4</sup>, R. López<sup>5</sup>, M.J. Martínez-Echevarría Romero<sup>6</sup>, C. Meléndez<sup>7</sup>, R. Michalczuk<sup>8</sup>, F. Mota<sup>3</sup>, D. Oravec<sup>9</sup>, I. Podadera<sup>1</sup>, Y. Qiu<sup>10</sup>, M. Ruiz<sup>1</sup>, A. Serikov<sup>10</sup>, M. Vázquez<sup>6</sup>, G. Wojtania<sup>11</sup>, A. Zsakai<sup>9</sup>, A. Ibarra<sup>1,3</sup>, the EUROfusion WPENS Team<sup>a</sup>

<sup>1</sup> IFMIF-DONES España, Granada, Spain

<sup>2</sup> Universidad de Castilla-La Mancha, Toledo, Spain

<sup>3</sup> CIEMAT, Avenida Complutense 40, Madrid 28040, Spain

<sup>4</sup> C3D, Budapest, Hungary

<sup>5</sup> Empresarios Agrupados, Madrid, Spain

<sup>6</sup> Universidad de Granada, Granada, Spain

<sup>7</sup> Esteyco, Madrid, Spain

<sup>8</sup> Warsaw University of Technology, Warsaw, Poland

<sup>9</sup> HUN-REN Centre for Energy Research, Atomic Energy Institute, Budapest, Hungary

<sup>10</sup> Karlsruhe Institute of Technology (KIT), Karlsruhe, Germany

<sup>11</sup> National Centre for Nuclear Research, Otwock—Świerk, Poland

E-mail: [santiago.becerril@ifmif-dones.es](mailto:santiago.becerril@ifmif-dones.es)

Received 1 November 2024, revised 31 May 2025

Accepted for publication 30 June 2025

Published 30 September 2025



## Abstract

The IFMIF-DONES test systems (TS) gather the experimental facilities offered by the plant, as well as the ancillary systems providing supplies and services both to those facilities and the irradiation modules, the latter ones belonging to the TS, although being excluded from the scope of this article. The irradiation modules gather any system that will be irradiated behind the lithium target inside the test cell (TC). Therefore, the TC also houses the liquid Li target and the stripping reaction held between the latter and the D+ beam. The TC is described in section 2, addressing as well some detail (section 2.1) about transversal key aspects like safety, RAMI, maintenance and others, although the safety aspects are collected in a dedicated part (section 5). The vacuum vessel is described in sections 2.2.1 and 2.2.3, relevant outputs from seismic, thermo-structural and fluido-dynamics analyses being as well provided. The shielding blocks are described in section 2.2.2, the lining part covering the building cavity filled in section 2.2.4, the floor in section 2.2.5, and the uppermost part in section 2.2.6. Section 3 is fully dedicated to the TSs ancillaries, a summary description being included for each of the subsystems, as well as an overview of their functional requirements. Section 4 provides a functional description of the different facilities for complementary experiments, apart from the TC. Section 5 is focused on safety issues applicable not only to the TC but to all the TSs included in the present article.

<sup>a</sup> See the Appendix in Ibarra *et al* (<https://doi.org/10.1088/1741-4326/adb864>) for the EUROfusion WPENS Team.

\* Author to whom any correspondence should be addressed.



Original content from this work may be used under the terms of the [Creative Commons Attribution 4.0 licence](https://creativecommons.org/licenses/by/4.0/). Any further distribution of this work must maintain attribution to the author(s) and the title of the work, journal citation and DOI.

Next, the current guidelines are given for the alignment (section 6) of the in-vessel systems and the integrated commissioning inside the TC (section 7). Finally, section 8 collects the main conclusions about the current status of the design of the TSs, irradiation modules excluded.

**Keywords:** IFMIF-DONES, fast neutron spectrum, vacuum vessel, neutron shielding, test systems, experimental facilities, safety confinement

(Some figures may appear in colour only in the online journal)

## Acronyms

AC	Access cell
ACPs	Activation and corrosion products
ASCE	American Society of Civil Engineers
AV	Accelerator vault
BP	Back plate
CP	Control point
DBA	Design basis accident
EPS	Electrical power system
FCE	Facility for complementary experiments
FPS	Fire protection system
GFM	Glass-filled magnet
GICS	Gas inventory control subsystem
GPS	Gas purification subsystem
G-RWTS	Gas radioactive waste treatment system
HCS-LP	Helium cooling subsystem–low pressure
HCS-MP	Helium cooling subsystem–medium pressure
HEBT	High-energy beam transport
HFTM	High-flux test module
HROC	Heavy rope overhead crane
HRS	Heat rejection system
HTO	Hydrogen tritium oxide
HVAC	Heating, ventilation and air conditioning
IFMIF-DONES	International fusion materials irradiation facility–DEMO-oriented early neutron source
INFN	Istituto Nazionale di Fisica Nucleare
IPA	Inlet plug access
ISRS	In-structure response spectrum
LICS	Local and instrumentation control system
LLC	Lithium loop cell
LN2	Liquid nitrogen
LSP	Lower shielding plug
L-RWTS	Liquid radioactive waste treatment system
LV	Low voltage
MB	Main building
NBS	Neutron beam shutter
NBT	Neutron beam tube
PASS	Personal access safety system
PCP	Piping and cabling plug
OPA	Outlet plug access
QTA	Quench tank
RAFM	Reduced-activation ferritic-martensitic
RAMI	Reliability, availability, manufacturability and inspectability
RAS	Reference-accident scenario
RBSB	Removable biological shielding block

RH	Remote handling
SBPs	Site, building and plant systems
SCS	Service control system
SGS	Service gas system
SICs	Safety-important components
SL	Seismic level
SPND	Self-powered neutron devices
STUMM	Start-up monitoring module
SWS	Service water system
TAA	Target assembly
TC	Test cell
TCCP	Test cell cover plate
TIR	Target interface room
TSs	Test systems
TSA	Test systems ancillaries
TSP	Top shielding plug
TSY	Target system
TWBD	Through-wall beam duct
USP	Upper shielding plug
WCS	Water cooling system

## 1. Introduction

The IFMIF-DONES plant is based on a linear accelerator providing a 5 MW, 125 mA D<sup>+</sup> beam –two beams in a later upgraded stage– hitting, in a continuous wave regime, a liquid lithium target. As a consequence, the resulting stripping reaction produces extremely intense radiation fields, both gamma and fusion-like fast neutrons.

Therefore, IFMIF-DONES will offer a variety of outstanding experimental capabilities with a special focus on fusion-related purposes. Nevertheless, those capabilities extend beyond fusion and reach other scientific areas.

The TSs collect a group of systems in charge of providing the appropriate conditions, environment and room in the irradiation facilities offered by IFMIF-DONES to the scientific community, as well as all the modules exposing payloads to the fusion-like irradiation fields produced in the core facility, the so-called TC. This group of key systems is composed by:

- The TC (figure 1), which provides the heavily shielded cavity where the stripping reaction takes place between the deuteron (D<sup>+</sup>) beams—one at an early phase of operation of the plant; two at a further upgraded phase– and the liquid lithium target.

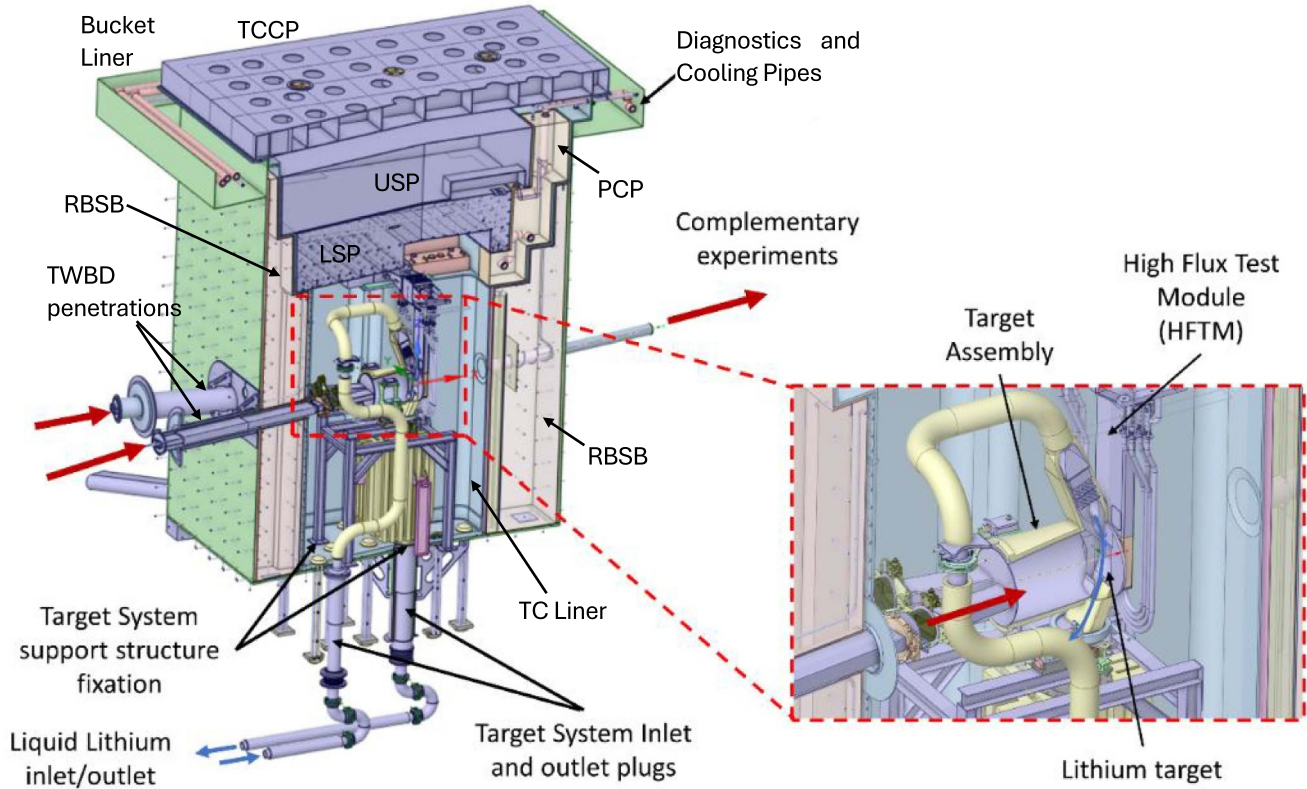


**Figure 1.** Test cell containing the target system and the high-flux test module. Reproduced from [1]. CC BY 4.0.

- Several irradiation regions [2] have been defined behind the TSY [3], depending on the neutron flux: between  $10^{14}$  and  $10^{15}$  n cm<sup>-2</sup>.s for the high-flux region; between  $10^{13}$  and  $10^{14}$  n cm<sup>-2</sup>.s for the mid-flux region; and below  $10^{13}$  n cm<sup>-2</sup>.s for the low-flux region [4].
- All the irradiation modules [5], which include all the systems that will be placed just behind the TSY inside the TC and will expose payloads to the neutron and gamma fields produced by the stripping reaction.

Amongst them, the HFTM is the first module that will be irradiated during the operation phase of the plant, its payload consisting of around one thousand miniaturized specimens made of RAFM steel.

Furthermore, another irradiation module, the so-called STUMM, is foreseen to play a key role during the last phase of the commissioning of the plant.

Apart from those, other irradiation modules will be installed in the TC during the different irradiation campaigns along the lifetime of the plant, thus taking advantage of all the irradiation regions available behind the TSY.

- The TSA, which play an intermediate role between the plant systems and the TS customers, thus providing the latter with the required services and supplies.
- The FCEs, which groups all the systems enabling the use of some specific rooms of the plant for experimental purposes:



**Figure 2.** Overall view of an excerpt of the main building where the TC is placed in the main building.

in particular, the room downstream from the TC and the room below the AV.

Figure 2 shows the location of the TC in the MB of the facility: behind the linear accelerator and above the lithium loop.

The present work describes the current, updated status of the design of the IFMIF-DONES TSs -except the irradiation modules [5]- as well as the associated main features applicable in terms of transversal areas like neutronics, maintenance, RH, safety, alignment and commissioning.



Finally, the arrangement of rooms related to the TS can be found in [6], as well as all the rooms around the TC, one of them being fully dedicated to the TSA.

## 2. The TC

### 2.1. Main functional and safety requirements

The TC [1] is the system that provides the core irradiation facility at IFMIF-DONES. Its main functional requirements include providing a secure containment structure for production of the stripping reaction and the neutron and gamma irradiation fields. Therefore, it must provide the space for safely housing the TSY and the irradiation modules that will expose payloads to those fields. From now on in the present article, all those systems may be called in-vessel systems.

Furthermore, the TC must be heavily shielded to fulfill with the dose rate levels allowed in the adjacent rooms (figure 3), in accordance with the applicable safety classifications to ensure the safety of personnel access and machine safeguarding.

Ten  $\mu\text{Sv h}^{-1}$  is the value that has been taken as a requirement for the design of the shielding components, including components from the TC and the MB. Of course, the rooms having thru-all penetrations towards the TC cannot preserve this low dose rate value, so they have been properly classified (red areas) to avoid personnel access during operation. Nevertheless, as a best practice, the shielding thicknesses around the TC have been homogenized by following the design consistent with the most stringent requirement ( $10 \mu\text{Sv h}^{-1}$ ). Figure 3 shows the shielding performance of the current design, which is consistent with the threshold mentioned above.

The TC is very strongly constraint by crucial top-level requirements from safety and RAMI. On one side, the overall plant's availability shall be higher than 70% while the plant's lifetime shall be longer than 30 years. On this regard, the current baseline considers two yearly periods for regular maintenance: one short of 3 d and one long of 20 d. This strong requirement in terms of availability poses high quality requirements for all the lifecycle phases of the TC.

On the other side, the TC takes part in the first safety confinement barrier (figure 4) of the plant in case of eventual release of ACP as well as activated lithium impurities, e.g. Be7 and tritium. In particular, the TC components (figure 1) that belong to this safety confinement barrier are the TC liner and the TCCP, which confer together a vacuum vessel enclosing the inert He-based atmosphere at 90 mbar (working pressure) to the components and systems housed inside. As a safety mitigation in case of leakage, the strong negative pressure differential w.r.t the pressure outside the TC liner will prevent ACPs from being released outwards so the eventual leaks would become rather inflows being captured as a pressure increase inside the vessel.

To keep the activation produced by the interaction with the fast neutron fields as low as possible, the gas species selected for the atmosphere inside the TC liner is helium. In addition, the level of pressure has been defined as 80% of the pressure

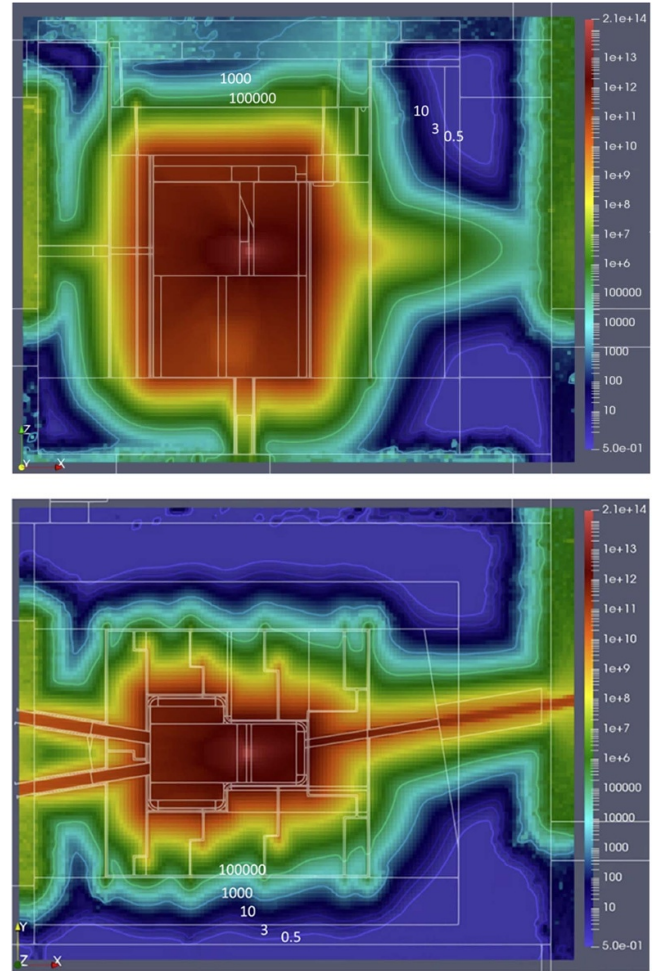


**Figure 3.** Vertical (top) and horizontal (bottom) sections of the dose rate maps inside the TC and its surroundings. Few spots need to be fixed in the baseline design to avoid local streaming. Reproduced from [7]. CC BY 4.0.

existing on the BP of the TSY under working conditions, as well as under all the transitional states previously run from atmospheric conditions. Thus, in case of eventual BP breakage, the lithium spillage would go outwards from the TSY) preventing any damage due to lithium inflow upstream into the accelerator beam lines and hardware.

As the TSY and the irradiation modules will be housed inside the TC liner, the TC must enable, through the TWBD penetrations, access for the deuteron beam pipes. Likewise, specific penetrations enable the continuity between the lithium inlet/outlet pipes and the lithium loop in the room below (LCC). Very importantly, all these penetrations belong as well to the TC liner and take also part from the first safety confinement barrier, so they need to follow high quality standards as well.

The use of fluids inside the TC liner is driven by risk mitigation in case of lithium spillage inside the vessel. Consequently, the use of water for cooling the in-vessel components is strictly forbidden. Indeed, a highly exothermal reaction would take place in an event leading to contact between water and liquid lithium.

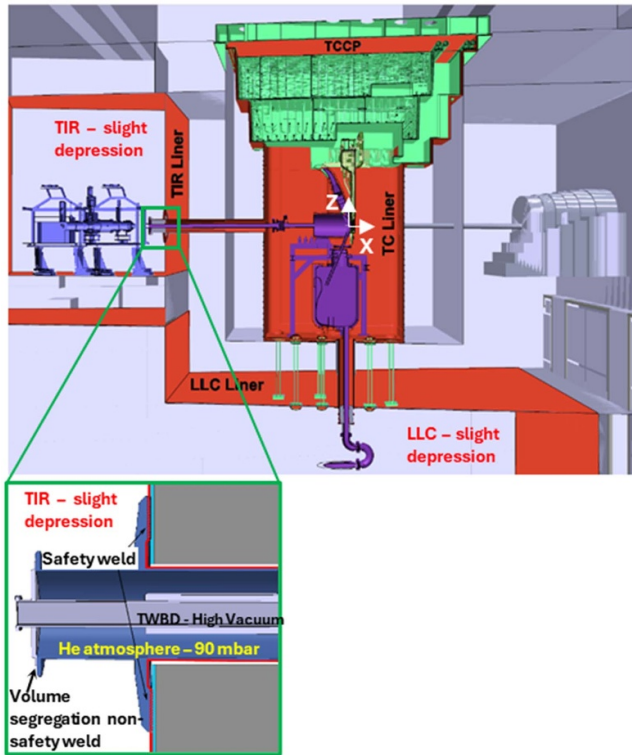


**Figure 4.** Top: first safety confinement barrier around the TC area, which includes the TC liner, the TCCP and, and by means of proper penetrations, the liners of both the target interface room (TIR) and the lithium loop cell. Left: detail of the interface between the TIR and the TC liner. Red-colored boundary depicts the first confinement barrier. Note that the weld segregating the TIR (slight depression atmosphere) from the TC liner (He at 90 mbar) is not a safety boundary. The same concept applies to the penetrations towards the lithium loop cell (LLC).

Quite importantly, the lithium fire inside the TC is considered a beyond-design basis scenario because of the inertized concept of the confinement safety barrier-He inside the TC; Ar inside the TIR and LLC (figure 4). Anyway, according to [8], the ignition temperature of liquid lithium is in the range of 400 °C–600 °C for moist air while the temperature of the liquid lithium flow running through the inside of the TC liner is 300 °C, well below the range above mentioned.

The strong requirements applicable to the TC coming from safety are closely followed by the seismic requirements to be fulfilled by the main components of the TC. This means that the first safety confinement barrier must be preserved even in the case of a seismic event SL-2 (design basis earthquake) while the mechanical integrity for quick re-start of the TS systems must be preserved in case of a seismic event SL-1 [9]. In the scope of the present article, more detail is given concerning the performance of the TC liner under a SL-2 event since it is a worst-case scenario (section 2.2.3.4).

From structural standpoint, the TC must also provide stable and reliable mechanical interfaces for the placement of the in-vessel systems, the mechanical shifts from alignment conditions-room temperature and atmospheric pressure-to working conditions being limited around 2 mm.



**Figure 5.** Layout of all the RBSBs providing the cavity for the TC liner. Red highlighted values are the integrated nuclear heats (kW) per each RBSB.

From maintenance point of view, the TC must also observe consistency and appropriate interfaces with RH means for all those maintenance procedures that cannot be implemented either hands-on or hands-off. To be compatible with the availability requirements, the design of the TC is driven to minimize the RH-based maintenance procedures.

Last but not least, the current TC baseline concept is strongly driven by its maintainability requirement, which, on the contrary to the former monolithic concept, has led to a layout of individually RBSB that can be replaced in case of serious failure. Likewise, this philosophy has been applied to the TC liner, which is placed in the inner cavity conferred by the RBSBs (figure 5). It is assumed that replacing one of those massive components will imply a long shutdown of the facility, which leads again to very high requirements in terms of quality standards for those components, with special attention to their cooling circuits and leak-tight weld beads.

## 2.2. Technical description

The main components of the TC are shown in figure 1.

**2.2.1. The TCCP.** The TCCP, made of stainless steel AISI316L, provides, together with the TC liner, the leaktight enclosure under helium-based, rough vacuum atmosphere. The TCCP is the detachable part when the TC needs to be open for maintenance reasons. The joint between the TCCP and the TC liner is kept sealed by means of a gasket against the uppermost rectangular perimetral flange of the latter.

The TCCP is designed to take advantage from its envelope for shielding purposes. Since nuclear heating is quite low at this region of the TC, the shielding material to fill the TCCP will be polyethylene.

**2.2.2. The shielding components.** The main shielding components of the TC are the TSPs, the PCPs and the RBSBs.

Each of them consists of a steel-lined block filled with heavy concrete, where the concrete does not play any high structural function because it must withstand only its self-weight. This is a conservative approach such that any eventual degradation of the concrete [10] may not have impact on

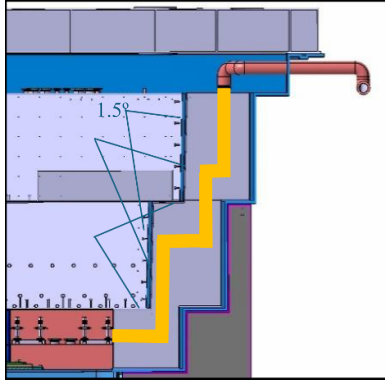


**Figure 6.** Vertical cut detail showing the clearance between the TSPs and the inner surfaces of the PCPs. The angle of  $1.5^\circ$  applied to the lateral sloped surfaces of the TSPs is also shown. The same concept (not shown here) is applied to the gaps between the TSPs and the inner surfaces of the TC liner. The USP presents a pocket on the lower part to enable room for the inlet/outlet connections (not shown) for the He cooling of the LSP.

the structural performance of the TC, in sight of the very high neutron fluxes produced. Therefore, the inside of the shielding block must include the proper structural features to prevent the concrete from being subjected to significant tensile stresses that may lead it to cracking during the component's lifecycle.

Both the TSPs and the PCPs (figure 1) are mechanically supported by the TC liner while the RSBs are placed outside and sit on the bucket liner floor.

The geometry of all these shielding components contributes to a high rate of material filling and shielding against the neutron streaming towards the adjacent rooms. This translates into a definition of gaps constrained by a reasonably small clearance for assembly of adjacent components. Consequently, both the shielding components and the TC liner follow intricate, bespoke, doglegged shapes. The current baseline design, therefore, includes gaps of 40 mm between adjacent RSBs, around 60 mm between RSBs (figure 6), and the bucket liner, and around 70 mm between the RSBs and the TC liner outer surface. Regarding the TSPs, the respective gap between each TSP and the PCPs inner surfaces is 40 mm (figure 6) which is the same of the TSPs w.r.t the TC liner inner surfaces.

At present, this baseline is considered quite reasonable as a good balance between shielding and feasibility in terms of manufacturability and assembly. Nevertheless, a more accurate study will be developed during the next steps of the project to fully ensure the feasibility of the design from all standpoints.

**2.2.2.1. The TSPs.** Once the TCCP is removed, the TC liner is only visible by means of its uppermost rectangular perimetral flange, the TSPs being, at this moment, fully accessible. The largest plug is the USP, which contributes, together with the LSP to the shielding upstream to the room above the TC (figure 3) the AC, where human presence must be enabled while the operation in the TC is being carried out.

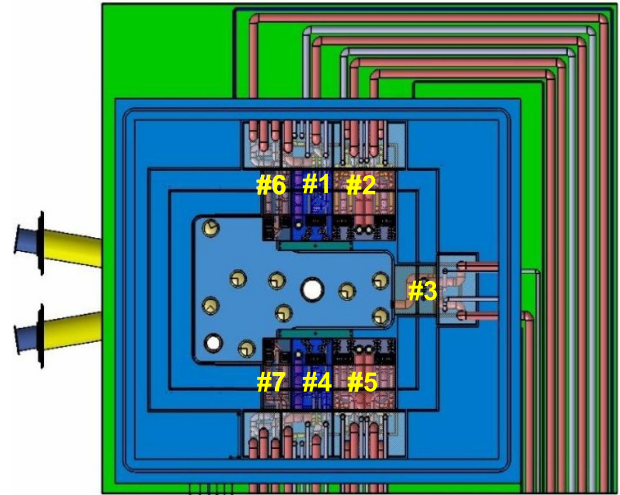


**Figure 7.** View of the TC liner inside showing the numbering of the PCPs: #1 and #4 for the HFTM [5] and the STUMM [5], #2 and #5 for other irradiation modules [5], #3 for the TC liner, and #6 and #7 for the TSY. In addition, a tentative notion about the routing of all the pipes and ducts outside the TC liner is given. The bucket liner needs to be enlarged, at its uppermost part, along two sides in order to drive all the ducts and pipes outside the TC liner.

According to the present baseline concept, the USP-around 120 Tm-is the heaviest component to be handled by the HROC in the AC [11].

The geometry and concept of the LSP, just below the USP, are similar to the latter, the main difference being its much higher exposure to the neutron fields, which leads to a helium-based cooling flow for proper evacuation of the nuclear heating. In order to avoid any risk of exothermal reaction, the LSP is cooled by helium. These RH inlet and outlet helium connections will be located on the upper surface of the LSP so a pocket (figure 6) is needed at the lower part of the USP to enable room for them.

In order to enable proper insertion to and extraction from the TC liner, each of the TSPs has its lateral surfaces convergent with  $1.5^\circ$  angle (figure 6).

**2.2.2.2. The PCPs.** Apart from the TSPs, other essential shielding plugs are the PCPs, which, in addition, allow the transport of all the signals, power supply, as well as several gas and vacuum services, required by the in-vessel systems and the TC liner atmosphere during all their operational and maintenance states. Therefore, each PCP (figure 8) has got, embedded in the concrete, a complex network of pipes for gas/vacuum transport and ducts for electrical harness. Those features must also follow complex, dogleg-shaped geometry to avoid neutron streaming. The PCPs numbering is shown in figure 7. The TSY is serviced through PCPs #6 and #7. PCPs #1 and #4 provide services and supply to HFTM while PCPs #2 and #5 do so for other irradiation modules behind the high-flux region. Pipes and ducts from PCPs towards the corresponding feedthroughs at the TC liner walls go as short as possible and orthogonal to the wall where they exit. The failure probability for this hardware inside the TC liner is minimized, which



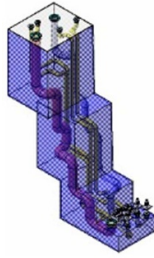


**Figure 8.** Detailed view of one of the HFTM PCPs according to the current baseline design.

is also better from availability standpoint since maintenance tasks outside the TC liner do not require opening the TC, so they will be probably quite shorter.

**2.2.2.3. The RBSBs.** Together with the TSPs and the PCPs, the neutron shielding performance required by ensuring the safety classification of adjacent rooms is completed by the RBSBs [7] and the MB structure (figure 3).

The RBSBs include the removable shielding blocks filling the space between the bucket liner and the inner cavity of the TC where the TC liner is placed.

The current baseline includes 11 RBSBs (figure 5). Since they are placed outside the TC liner, the RBSBs requiring cooling to evacuate significant nuclear heating -all of them except RBSB#9 and RBSB#10- will use water as cooling fluid because no contact with lithium can happen in case of failure. In the case of the TSPs, which are placed inside the TC liner, the stainless-steel liner prevents any incidental contact between spilled liquid lithium and concrete.

The cooling circuits are parts with higher probability of failure within a RBSB. To reduce this as much as possible, the length of seamless pieces will be maximized for the circuit pipes.

The RBSBs, together with all the removable shielding components, are foreseen to be filled with heavy concrete [12]. Dose rate maps shown in figure 3 consider heavy concrete for all the removable shielding components and ordinary concrete for the MB structure.

### 2.2.3. The TC liner

**2.2.3.1. General description.** The TC liner is the most critical component of the maintainable, leaktight vacuum vessel where the PCPs, the TSPs and the in-vessel systems-TSY and irradiation modules- are placed, the stripping reaction in a continuous, steady-state being held thanks to the interaction between the 140 MeV, 125 mA, continuous-wave (CW) deuteron beam (or beams) and the liquid lithium target.

Apart from the TC liner main body, such a vacuum vessel is composed of:

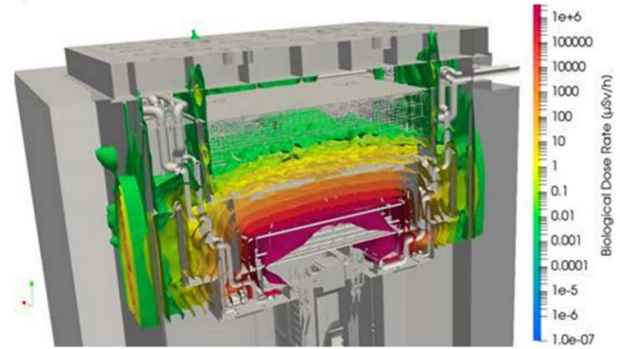


**Figure 9.** Detail of the residual dose rate map of the uppermost part of the TC. Residual doses coming from the TC liner, the HFTM, the TA and QT are included. Biological dose rates much lower than  $10 \mu\text{Sv h}^{-1}$  are expected above the USP so hands-on tasks seem quite feasible.

- the TCCP, which provides leak tightness at the top of the TC,
- the penetrations enclosing the TWBDs; and
- the penetrations enclosing the liquid lithium IPA and OPA and all corresponding closure weldings.

All these sub-parts are foreseen to be made of stainless steel 316 L.

While being conceived and designed for all the lifecycle of the plant—30 years at least- the maintainability requirement has led to a removable component so all their interfaces with the rest of the TC and with the MB structure are reasonably easy to cut-and-weld for eventual extraction in case of a serious failure.

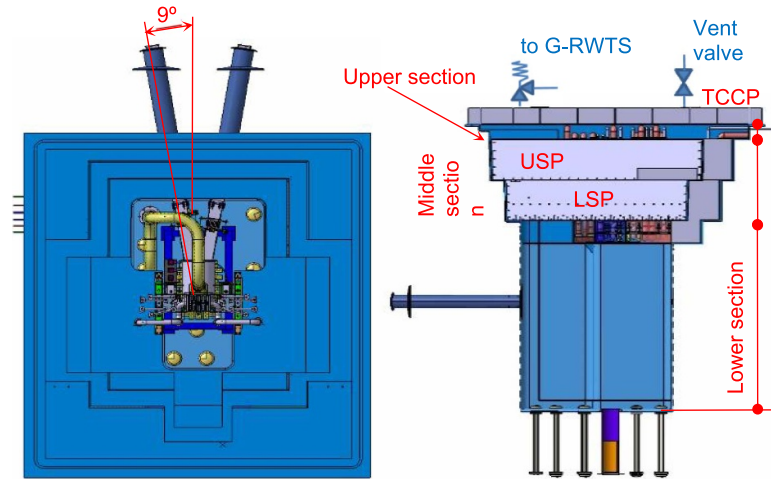
For the first installation, the penetrations are foreseen to be mounted from the TIR towards the TC, once the TC liner main body is placed and then welded hands-on to the latter.

Figure 9 shows the general geometry of the TC liner. In vertical direction, several main sections can be distinguished. At the bottom, the lower section keeps the geometry of the cavity where the in-vessel systems and components are placed and where the different irradiation regions are available for irradiation modules, just behind the TAA (figure 1). This volume is around  $60 \text{ m}^3$ . Its T-shaped envelope includes an area where the TSY, with its relatively big components are placed (QTA and TA), as well as the TWBD penetrations following the accelerator's beamlines with a convergence of  $9^\circ$  w.r.t the symmetry XZ plane (figure 9).

Just above the lower section, the middle section provides the proper interfaces for the mechanical seats of the TSPs inside the TC liner. The lateral clearances between TSPs and TC liner (40 mm), as well as those between each TSP seat and the PCPs (figure 6), allow for easy mechanical assembly of the plugs and appropriate pressure equalization between the upper and the lower sections.

At the top of the TC liner, above the USP, there is the upper section, which has a volume around  $20 \text{ m}^3$ . Its height is





**Figure 10.** Left: Top view of the TC liner showing the convergent TWBD penetrations. Right: vertical cut showing the TC liner sections, the TSPs, the PCPs and the TCCP.

constraint, on one side, by the upper surface of the USP and, on the other side, by the lower surface of the TCCP. This section includes the uppermost, large flange of the TC liner, which interfaces with the TCCP by means of a series of bolted joints -not yet included in the current baseline- and a sealing gasket, all of them accessible by hands-on maintenance procedures. Very importantly, the shielding performance of the USP and the LSP must provide residual dose rates low enough to allow hands-on procedures, once the TCCP is removed, concerning all the hardware above the USP, which includes all the ducts and pipes running inside the TC liner upper section from the PCPs to the feedthrough panels. Figure 10 shows the residual dose rate distribution in the upper section of the TC liner, which is below  $10\mu\text{Sv h}^{-1}$ .

Figure 7 gives an idea about the quantity of pipes and ducts running inside the upper section of the TC liner from the PCPs to the feedthrough panels (not shown). For each pipe or duct coming through the TC liner, a single feedthrough is needed, which, in turn, must be leaktight. All the single feedthroughs will be grouped in several feedthrough panels located in front of each PCP, such a way that no overlap between pipes/ducts exiting from different PCPs are foreseen inside the TC liner.

Feedthrough panels avoid direct interface between the feedthroughs and the TC liner main body so, in case of a leaky or faulty feedthrough, intervention on the TC liner main body is avoided. Obviously, the feedthrough panels must be easily detachable from the TC liner main body by hands-on means.

The central area of the upper section is kept empty to avoid any collision with the extraction/insertion of the TSPs.

The TC liner sections above the lower one do follow the stepped, doglegged shapes because, on one hand, they support the TSPs and, on the other hand, its external lateral surfaces face the RBSBs geometry. This very intricate shape of those sections of the TC liner poses additional difficulties from the manufacturing point of view. This must be considered in terms of mechanical tolerancing on those middle and upper sections to define properly the gaps w.r.t the RBSBs and avoid any

mechanical collision while avoiding any significant neutron streaming towards the AC.

**2.2.3.2. The TC liner atmosphere.** Concerning the atmosphere inside the TC liner, helium is foreseen as a residual gas in working conditions, i.e. 90 mbar. The leakage rate currently specified for the vessel is around  $3 \cdot 10^{-2} \text{ mbar l s}^{-1}$  although in the state of the art, similar or even bigger vessels with leak rates several orders of magnitude lower have been successfully built. Upon the start-up of the facility, the following stages are foreseen for carrying the TC liner from atmospheric conditions to working conditions:

1. Air removal by means of a vacuum cycle to reach 1 mbar.
2. Filling with helium gas to reach atmospheric pressure.
3. Vacuum pumps start-up to reach 90 mbar.

To drive the TC liner from working to maintenance conditions at atmospheric pressure, the opposite procedure is implemented although the TC liner volume is not filled with air but with argon to keep an inert atmosphere in presence of eventual lithium spills or remains.

All the management, monitoring and troubleshooting of the TC liner atmosphere will be driven by the corresponding TSA subsystem (section 3), i.e. the GICS. In particular, gas extraction is provided by a vacuum flange located on PCP3 (figure 6), vacuum being primarily provided to the lower section volume. The pressure in the different volumes inside the TC liner needs to be monitored, i.e. the upper volume and the lower volume. In addition, a venting valve is foreseen (figure 9) to equalize the pressure inside the vessel and outside, so any pressure differential affecting the TCCP is cancelled during its removal/insertion. Due to the large area of the TCCP, even a slight differential may induce high forces on the TCCP, its removal being compromised.

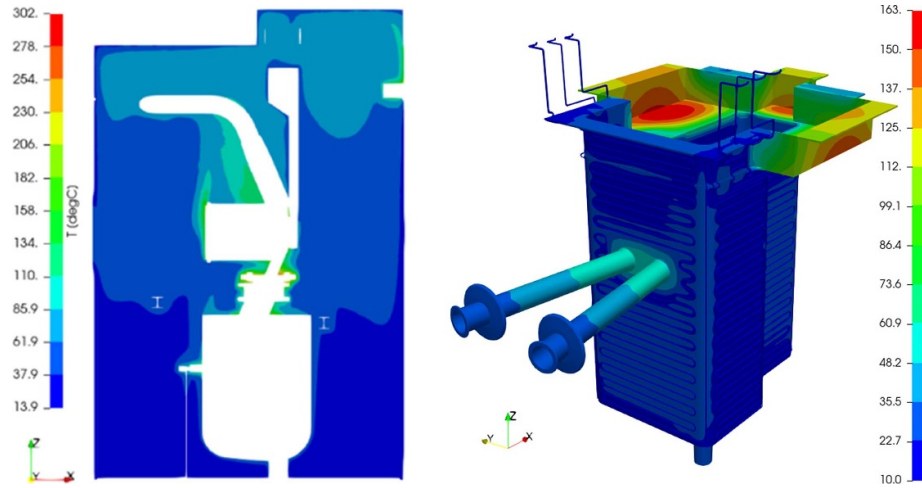


**Figure 11.** Left: temperature distribution map of the TC liner atmosphere. A convective plume can be seen, its maximal temperature being around 130 °C. Right: temperature distribution on the walls of the low section and some portion of the middle section of the TC liner. Water cooling keeps the low section mostly around 30 °C, the uncooled interface part of the TWBD sleeve penetrations being around 60 °C. The uncooled lower steps of the middle section get quite warm so a further evolution of the design should include cooling for those.

The temperature required for the atmosphere inside the TC liner is 50 °C–60 °C, its main contributor in terms of cooling being the TC liner water circuits. Anyway, an additional cooling capacity backup is provided by the GPS from the TSA (section 3) if necessary.

The TC liner is cooled by three water circuits in parallel ( $0.91 \text{ s}^{-1}$ ), the heat power to be dissipated being 28 kW in total, 17 kW from nuclear heating and 11 kW from heat coming from in-vessel components and atmosphere. A convective plume - maximal helium speed of  $1.4 \text{ m s}^{-1}$  is produced around the BP and the HFTM, its maximal temperature reaching around 130 °C (figure 11). Nevertheless, the average temperature of the atmosphere is around 46 °C, which is consistent with the requirement.

The TC liner low section is kept around 30 °C–40 °C, well within the requirement of 50 °C–60 °C as maximal temperature (figure 11). Nevertheless, a further evolution of the design must include cooling for the lower steps of the middle section since they heat up as much as 160 °C.

**2.2.3.3. Thermo-structural analyses.** From structural point of view, several mechanical supporting layouts were analyzed with special focus on their performance against the seismic events applicable and the reliability and stability of the key mechanical interfaces for the in-vessel components position. The mechanical supporting layout providing the best mechanical performance in the models is based on a very rigid attachment of the bottom of the TC liner to the Bucket floor, as well as the attachment at the uppermost part of the TC liner. The structural behavior of such a concept against the seismic loads is described in the next section.

Concerning the mechanical stability for the in-vessel components, an important topic comes from the need for the in-vessel components to not have extremely high displacements from alignment to working conditions. Those displacements have been, at a first approach, required to be around 2 mm

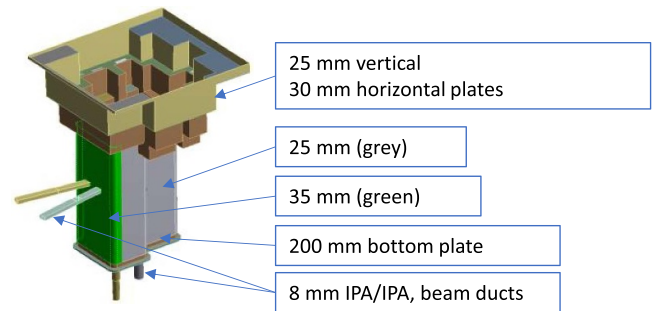


**Figure 12.** TC liner model showing the wall thicknesses considered for FEA analyses.

maximum. The alignment (section 6) will be implemented at atmospheric pressure and room temperature while, at working conditions, the TC liner will be at 90 mbar and subjected to a thermal gradient resulting from the steady state determined by the nuclear heating and the performance of the cooling systems involved (figure 11).

Figure 12 shows the model subjected to analyses -gravity, thermal and vacuum loads- with the thicknesses considered for all the plates of the TC liner. Thermal loads are considered in the model as the temperature field distribution on all the parts of the TC liner resulting from previous thermal analyses, which are addressed later in the present section.

Maximal deformation (25.2 mm; figure 13) is obtained in one of the longest plates of the main body. Nevertheless, this area is far away from the key mechanical areas inside the TC liner, e.g. where the TA and the HFTM are mechanically supported. According to the present models, the displacements, from alignment conditions (atmospheric pressure, room temperature) to working conditions, for those key in-vessel systems, are shown in table 1.

Even if further analyses will be implemented, as long as the design is getting to its final stage, these results are quite

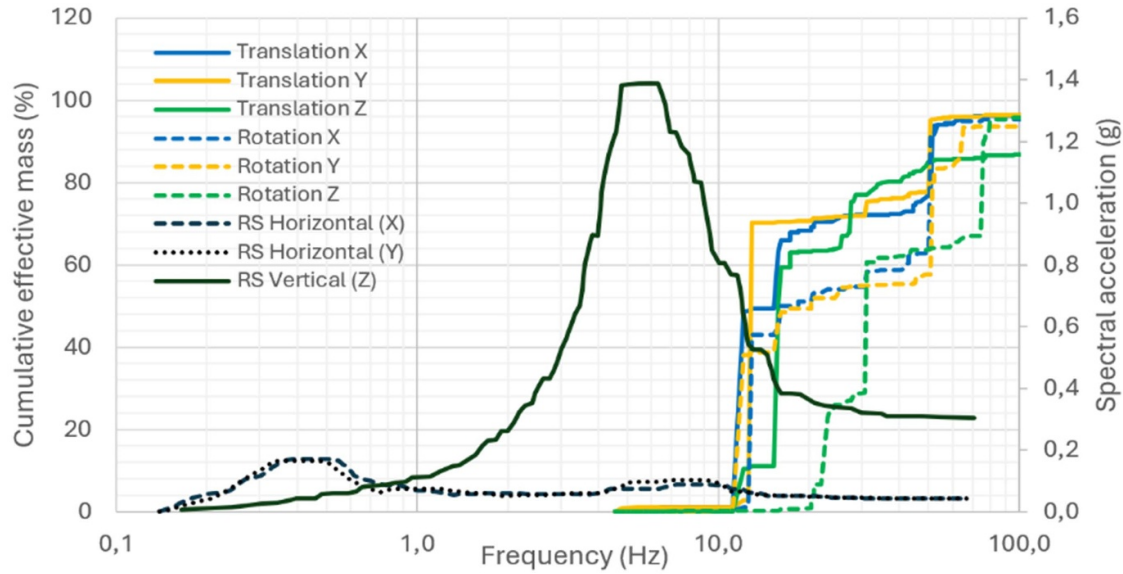


**Figure 13.** ISRS for design earthquake (SL-2), horizontal and vertical, corresponding to the location of the test cell in the main building (4% damping) and modal analysis results: effective cumulative mass of the structure, translation and rotation for the TC liner.

**Table 1.** Displacements of the TAA and HFTM from alignment to working conditions.

TA displacements (mm)			HFTM displacements (mm)		
X	Y	Z	X	Y	Z
0.1	0.01	≈0	0.43	−2.20	0.03

promising because the distortion after the alignment of the in-vessel components will be kept very low.

**2.2.3.4. Seismic analyses.** At present, the seismic analyses have been focused on the TC liner because it is the most critical and demanding component amongst the TS. For the rest of seismically-required TS components, dedicated structural analyses are yet to be implemented. Since the TC-liner is classified as seismic class SC1, its function as part of the first safety confinement barrier must be kept in an event of a SL-2 earthquake, which is the design-basis earthquake.

Figure 14 shows the ISRS for a SL-2 earthquake corresponding to the location of the TC. There is a strong difference between the horizontal and vertical spectra, due to the base isolation of the MB [9]. This isolation reduces the horizontal natural frequencies of the MB [13], causing an amplification in frequencies below 1 Hz and drastically reducing the accelerations above 1 Hz, for horizontal motion. For vertical motion, the isolation does not have the reducing effect and may even amplify accelerations [14]. This is the main reason why vertical seismic demand governs in this case seismic analyses.

The dynamic behavior of the TC is strongly influenced by the shielding concrete masses resting on the TC liner (USP, LSP and PCPs), currently estimated to weigh around 250 tons. The seismic analyses here presented already consider the mechanical supporting layout -top and bottom anchoring- described in section 2.2.3.3. The anchoring layout considered for the attachment of the bottom plate to the bucket liner floor

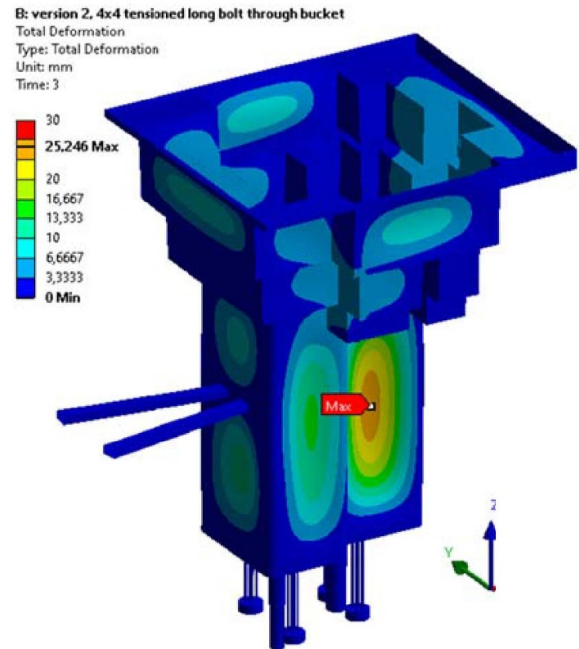


**Figure 14.** Deformations of the TC liner under gravity, thermal and vacuum loads.

consists of 11 spots (see section 2.2.5) each of them indicating the local action of corresponding pre-stressed bolt. For the upper fixation, a rigid connection, with restricted displacement and rotation, between the uppermost flange of the TC liner and the bucket liner has been considered (figure 15). A dedicated



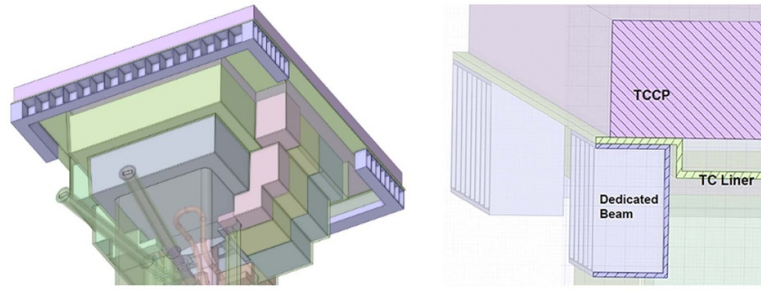


**Figure 15.** Upper boundary conditions considered for the TC liner seismic analyses.

beam to provide high bending momentum has been considered all along the uppermost perimeter of the TC liner, except for the sections where pipes and ducts come out from the PCPs and go outside the TC liner. The TSP masses have been also considered through friction contact (0.2 as friction coefficient).

The results of the modal analysis can be seen in figure 14. The modal analysis is prestressed, performing a previous static analysis considering the operational loads: gravity, thermal loads and the negative internal pressure of the vessel, around 0.1 MPa. The main modes of horizontal translation are between 11 and 13 Hz, as is rotation around the horizontal axes. Vertical translation mobilizes most of the mass between 15 and 16 Hz. Rotation around the vertical axis has its main modes above 20 Hz. By comparing the modal results with the spectra, the accelerations to which the main modes are related are close to the tail of the spectra, i.e. the zero period acceleration (ZPA). Quite reasonably, the maximum acceleration corresponds to the translation in the vertical axis, around 0.5 g.

With these modal results, a response spectrum analysis was performed. Results on the three axes have been spatially combined with the Newmark combination (ASCE, 2019). The results of the response spectrum analysis are combined with the static ones to obtain the total demand on the structure considering the operating loads and the design earthquake. The local primary membrane stress results, combined from the static and response spectrum analysis can be seen in figure 16 for the most demanding combination. The maximum allowable local primary membrane stress for annealed AISI316L under TC liner operational conditions (temperature, negligible irradiation damage) is 220 MPa according to RCC-MRx [15]. The structure presents certain areas where relevant stresses appear ( $\sim 210$  MPa), mainly around the sharp corners and the vertical plates at the bottom part of the vessel.

In general, the structure presents an acceptable seismic behavior from the design point of view. Since the seismic inputs are not yet definitive (the ISRS are not yet consolidated), special attention should be paid to their evolution, especially for vertical motion.

**2.2.4. The bucket liner.** The bucket, which is made of ordinary concrete, is the area of the MB structure that provides the big cuboidal cavity that is filled with the TC components. It

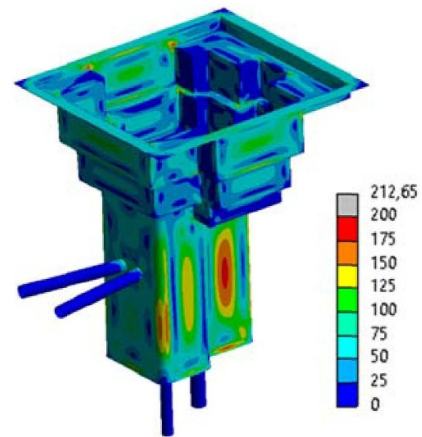


**Figure 16.** Results of the response spectrum analysis combined with the operating loads (Newmark combination, worst case). General primary membrane stress (von Mises)—MPa.

plays a key role in the shielding of the radiation coming from the stripping reaction to the adjacent rooms (figure 3).

The bucket liner covers the bucket with a thin layer made of stainless steel that prevents the contact between the MB concrete with water in case of an eventual spillage from the cooling circuits of any of the water-cooled components of the TC. In addition, it includes some draining channels (figures 17) at the bottom to drive the activated water from an eventual spillage to a tank embedded in the concrete of the TC floor.

Its uppermost part provides mechanical support for the attachment of the TC liner at the top as well as housing the path to the respective rooms of all the pipes and ducts providing services to the different TC components (figure 7).

**2.2.5. The TC floor.** The TC floor is composed of the stack of the TC liner floor, the bucket liner floor and concrete slab that separates the TC from the LLC. It plays a key role in the maintainability of the TC because it is the only part requiring water cooling that cannot be dismantled, so no circuits can be embedded in the concrete of the MB structure.

Therefore, its heat sink must be provided through the cooling elements of a detachable component, in this case the TC liner. The thick bottom plate of the latter has the cooling pipes welded on the outer surface and is in contact with the bucket liner floor by means of 11 spots (figure 18), each of them

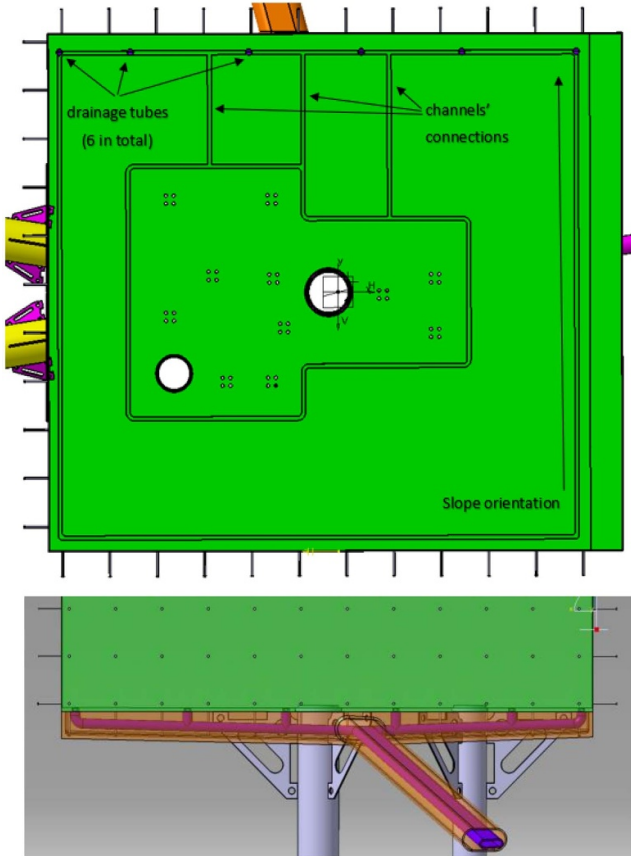


**Figure 17.** Top: view of the bucket liner showing draining channels on the floor. Bottom: front view of the lower part of the bucket liner showing the collector and drainage lines embedded in the MB structure concrete.

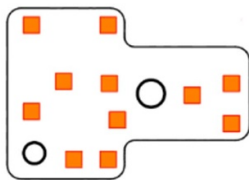


**Figure 18.** Tentative layout of the contact spots between the TC liner floor and the bucket liner floor, which has been considered for the bottom anchoring for the seismic analyses (section 2.2.3.4).

including pre-stressed long bolts through all the stacked components until the LLC liner.

The main aim of this highly hyperstatic layout is to provide significant thermal contact surface, so a soft interlayer material with high thermal conductivity will be needed, for eight of the 11 spots, in the interface between bucket liner floor and TC liner floor, the remaining three spots providing the kinematic mechanical constraints to the position of the TC liner on the bucket liner.

Besides this, maximizing the contact area between the bucket liner floor and the concrete below is crucial to minimize the heat power deposited on the concrete. On this regard, a thick bottom plate of the TC liner goes in the same direction. After dedicated neutronics analysis, a thickness of 100 mm

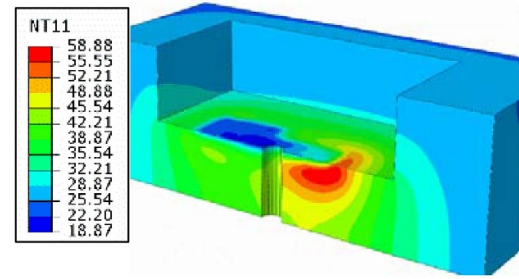


**Figure 19.** Temperature distribution on the TC floor and the bucket concrete.

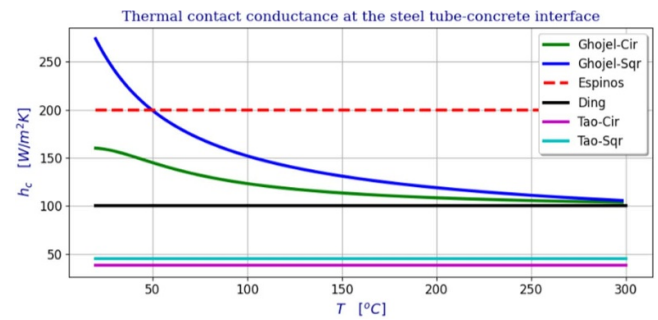


**Figure 20.** Thermal conductance between steel and concrete as a function of temperature based on different research works [16–20].

for the bottom plate of the TC liner has been considered the best value as a good compromise between the heat deposition (1.2 kW) in the concrete and the manufacturability and feasibility of the supply of the raw material. By doing so, active cooling of the bucket concrete is avoided, which would be a major issue from the availability point of view of the plant in case of serious failure.

Figure 19 shows the temperature distribution obtained in the bucket concrete by assuming that the bucket liner and the concrete is fully in contact in the areas with higher heat deposition. This will lead to clever techniques during the construction of the MB, e.g. using the bucket liner floor as permanent formwork structure for the concrete pouring of the slab, to ensure chemical adherence -and good thermal conductance- between the liner and the concrete.

Thermal conductance between both components is the dominant factor to keep the maximal temperature in the concrete below a reasonable value (around 60 °C).  $1.7 \text{ W m K}^{-1}$  has been assumed for the thermal conductivity of the concrete while  $70 \text{ W m}^2 \text{ K}^{-1}$  is the thermal contact conductance between the bucket liner and the concrete for the spots aligned with the mechanical supporting areas of the TC Liner, and  $30 \text{ W m}^2 \text{ K}^{-1}$  outside these spots. A higher value has been selected for the contact areas aligned with the supporting spots of the TC liner since the higher pressure produced on them enhance the thermal conductance. Anyway, both values are on the conservative side: the one applying outside the spots is lower than the worst value found in literature (figure 20).

**2.2.6. The TC uppermost part.** Although the design of the uppermost part of the TC is currently ongoing, a group of needs has been identified as main drivers:

1. Space around the uppermost part of the TC liner for the routing of all the pipes and ducts required for servicing the TC liner, the RBSBs and all the in-vessel components and systems.
2. Hands-on access to all the pipes and ducts mentioned in the last point, as well as their associated hardware (valves, gaskets, gauges, etc...). This maintainability access must be enabled as well for the feedthroughs of the TC liner.
3. Upper mechanical supporting points of the TC liner to provide natural eigenfrequencies away from the resonant range according to the seismic spectra applicable.

An enlargement of the bucket liner at its uppermost part (figure 7) will enable space and feasible hands-on access for the different bunches of ducts and pipes, and all their associated hardware.

Concerning the third bullet, the design is ongoing although the concept shown in figure 15 provides a good structural performance against the seismic loads applicable whereas it is compatible with the exit of the ducts and pipes from the PCPs.

### 3. The TSs ancillaries

The TSA are in charge of providing all the required services to the TS, mainly the TC, the HFTM and the STUMM according to the current baseline. They are comprised of the GICS, GPS, WCS, HCS-MP, HCS-LP and the Electric Power Supply Subsystem (TSA-EPS). Simplified diagrams of all these subsystems, except for the TSA-EPS, are shown in figure 21, which does not include redundant elements for a better understanding.

#### 3.1. GICS

The GICS is comprised of multiple vacuum pumps and compressors that make it able to remove or supply the internal atmosphere of the TC (He for operation, Ar for maintenance), the HCS-MP or the HCS-LP. It interfaces with the TC through the GPS. With two sets of two vacuum pumps, it can remove the atmosphere of those customers and store it in a buffer tank. From this buffer tank the gases can be fetched back and be stored in bottles for eventual later usage. Moreover, to supply gas to these customers, the GICS feeds them either through the SGS [6] helium and argon lines, or through the bottles whenever the quality of the stored gas is good enough.

The first pair of vacuum pumps is dedicated to removing the initial atmosphere of the TC with  $208 \text{ m}^3 \text{ h}^{-1}$ , while the second pair ( $1.2 \cdot 10^{-3} \text{ m}^3 \text{ h}^{-1}$ ) is dedicated at keeping the vacuum level (90 mbar) under working conditions. Each pair of vacuum pumps is equipped with inlet filters. The compressors are the same in each pumping unit with  $30 \text{ m}^3 \text{ h}^{-1}$  and the buffer tank has a capacity of  $3 \text{ m}^3$ . There are four kinds of bottles that can be filled: the first one can store Helium from the HCS-LP, the second one helium from the HCS-MP or the

TC, one for argon from the TC and the last one for gas waste disposal, all gases being compressed at 200 bar. Additionally, in the case of overpressure downstream the high-pressure compressors or in the external supply line, the GICS is equipped with a guard vessel of  $1 \text{ m}^3$  which is connected to the G-RWTS [6].

Very importantly, the GICS is in charge of the continuous monitoring of the pressure inside the TC liner and start-up the secondary pump to reset the desired pressure values inside whenever the pressure level has become too high. It also monitors the on/off ratio of the secondary pump since it gives a good notion of the eventual degradation of the leak tightness of the TC liner.

Some of the key components are redundant for availability reasons: pumping groups, filters and buffer tanks.

#### 3.2. GPS

The GPS re-circulates continuously—ten times per hour— the He atmosphere inside TC liner as well as removing any unwanted chemical species or aerosols during operation and providing with a backup cooling capacity to remove heat from the TC liner if necessary.

The GPS is equipped with a redundant air blower ( $600 \text{ m}^3 \text{ h}^{-1}$ ) equipped with redundant inlet filter as well. Upstream from the blowers, the flow goes through the GPS purification unit. Downstream of the blower, a heat exchanger is placed to lower the temperature of the flow from  $60^\circ \text{C}$  to  $30^\circ \text{C}$ , that first temperature being reached as an addition of the heat load coming from the TC and the heat injected by the blowers. For that purpose, the GPS is also equipped with a dedicated closed water loop, equipped with a plate heat exchanger to cool down the water, two redundant compressors and a surge tank. The gas temperature at the outlet of the shell and tube heat exchanger is controlled by the temperature transmitter that regulates the control valve located at the cold leg of the water-cooling loop.

The purification unit includes adsorption columns filled with porous substances, zeolites, where the impurities are adsorbed at cryogenic temperatures ( $-196^\circ \text{C}$ ) using LN2. It is assumed that all the circulated gas is processed and therefore cooled down by the purification unit, the effective cooling power is  $5.8 \text{ kW}$  which is equivalent to  $1.4 \text{ m}^3$  per day of LN2. The present concept is under revision to try to reduce the LN2 consumption.

The GPS acts as a confinement barrier by the closure of the isolation valve located at the inlet and outlet of the interface with the TC. These isolation valves are redundant.

#### 3.3. Water cooling subsystem

The WCS circulates a flow of water through the outer surfaces of some components of the TC to remove heat from them and keep their required working temperatures: under  $95^\circ \text{C}$  for the RBSBs and around  $50^\circ \text{C}$ – $60^\circ \text{C}$  for the TC liner. The combined expected heat load is about  $90 \text{ kW}$ , which is dissipated by a flow rate of  $25 \text{ kg s}^{-1}$  and an inlet temperature of  $12^\circ \text{C}$ , the  $\Delta T$  being  $2.2^\circ \text{C}$ .



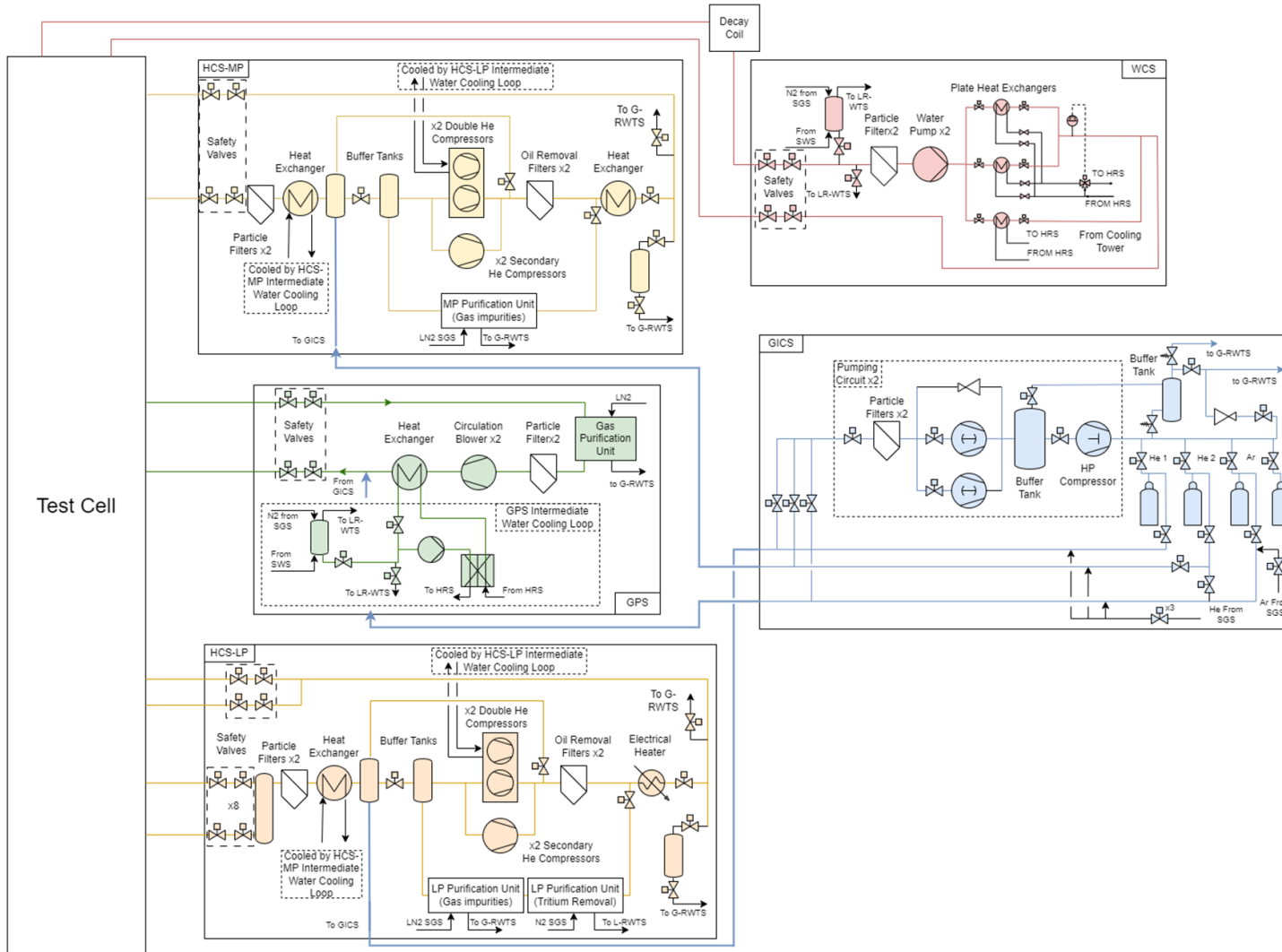


**Figure 21.** Schematic view of the test system ancillaries.

Two parallel heat exchangers are cooled with chilled water at 7 °C from the HRS [6] and, as a safety measure, there is an additional heat exchanger cooled by the HRS cooling towers (27 °C) in case chilled water is not available. In order to ensure that the temperature of the cooling water of the heat exchangers is appropriate, there is a three-way valve at the inlet of the heat exchangers, connected to a temperature transmitter that is located at the junction of both exchangers. The return line from the TC includes a decay volume -not yet defined- for the short half-life radionuclides ( $^{15}\text{O}$ ,  $^{19}\text{O}$ ,  $^{16}\text{N}$ ,  $^{17}\text{N}$ ) to decay under activity thresholds leading to activities below  $10 \mu\text{Sv h}^{-1}$ . On this regard, the water mass flow mentioned before is not yet consolidated since it is a key factor for the size of the decay volume. In the case of upgrading to IFMIF [2], having two accelerators, the thermal load would be double so the  $\Delta T$  will double but the same layout can be kept.

### 3.4. Helium cooling subsystems

The HCS-MP and the HCS-LP provide with helium flow the LSP and the HFTM or the STUMM, respectively. They both guarantee the supply of helium during normal operation and in case of electrical blackout. Additionally, the HCS-MP possesses a water-cooling loop dedicated to the helium/water shell heat exchangers of both HCS subsystems, while the HCS-LP has another dedicated water-cooling loop for the helium compressors of both subsystems.

The HCS-MP is designed to have a flow rate of  $0.28 \text{ kg s}^{-1}$  for a maximum heat load of 36.3 kW, with an inlet temperature of 20 °C and an outlet temperature of up to 44.7 °C. The HCS-LP is designed for a flowrate of  $0.36 \text{ kg s}^{-1}$  and a thermal load of 123.4 kW, with an inlet temperature of 50 °C and an outlet temperature of up to 116 °C.

Each HCS counts with 2 double compression units so 4 compressors in total. Under working conditions three compressors will be in use and one of them is on standby.

The configuration of both HCS is quite similar. The helium compressors have a filter in their inlets and can be isolated. Downstream, there are two redundant oil removal filters. After that, 2% of the flow rate is bypassed to the purification unit, which is similar to the one in the GPS, recirculating it to the buffer tank upstream the compressors afterwards. In the case of the HCS-LP, this bypass also involves a detritiation process. Upstream the compressors there are two pressure vessels, the first one connects to the purification system and the second one to the GICS system, both are equipped with pressure relief valves and pressure transmitters. Additionally, both systems have redundant filters at the outlets of their consumers to remove solid particles. And, lastly, both systems are equipped with guard vessels, located between the compressors and the consumer; they protect the consumer equipment from overpressure, the excess of pressure being discharged into it by a control system and/or safety relief valve.

Additionally, in case of electrical blackout, the HCSs can provide 2% of the nominal operation mass flow to remove decay heat from the TC for at least 3 d of operation using the

backup secondary compressors. These compressors are additional to the double compressors detailed previously.

In the HCS-MP, both upstream and downstream the compressors, there are shell and tube heat exchangers, the first for cooling down the helium coming from the consumer and the latter to compensate compression heat.

In the HCS-LP, there is only a shell-and-tube heat exchanger located upstream the compressors and downstream of them there is a heater, as the fluid needs to increase its temperature to the required one in the inlet of the HFTM. Also, another difference between both systems is that the HCS-LP collects all the returning lines -eight- coming from the HFTM in a vessel that controls the baseline mass flow and the pressure for the HFTM inlets. Each of the eight outlet lines from the HFTM includes a mass flow control valve to fine tune the needs of each of its eight cooling channels.

The HCS-MP will require a consumption of LN2 of  $1.7 \text{ m}^3 \text{ day}^{-1}$  while the HCS-LP will require  $2.2 \text{ m}^3 \text{ d}^{-1}$ . Additionally, upstream this purification unit, the HCS-LP has a detritiation unit, still in conceptual design, to remove radioactive gases generated during normal operation. It involves a detritiation process that will convert the tritiated chemical species (gaseous) into tritiated water. This design is divided into three different skids. The skid-1 is the detritiation system, where the helium flowrate passes through a pre-filter (to protect the detritiation equipment) and enters a catalytic reactor, where the tritiated gas is oxidized on a catalytic process using oxygen in the flow to convert the hydrogen and tritium chemical species to the oxide form (tritiated water, HTO). The inlet tritiated stream is mixed with dry air for optimal conversion of hydrogen/tritium species to the oxide form. This reaction is taken at high temperatures, so an electric heater is installed upstream the catalytic reactor. After the catalytic process, the helium flowrate is sent to an adsorption column, where the tritiated water vapor is adsorbed on molecular sieves columns operating under room temperature. The skid-2 has the function of performing the regeneration of the molecular sieves when they become saturated, dry nitrogen coming from the SGS is used in this process in counter flow through the beds, extracting the adsorbed water vapor, which is recovered afterwards in a condenser. The skid-3 collects the condensed water and pumps it to the L-RWTS.

Both HCSs have intermediates water cooling loops to cool down its own components. The HCS-MP intermediate loop cools down the shell and tube heat exchangers of both systems with water supplied at 12 °C and a flow rate of  $39.6 \text{ m}^3 \text{ h}^{-1}$ . While the HCS-LP intermediate loop cools down the Helium compressors of both with water supplied at 32 °C and a flow rate of  $34 \text{ m}^3 \text{ h}^{-1}$ .

Eventually, all the HCS water loops, as well as those from the GPS and the WCS, already consider connections to draining lines for eventual water removal towards the L-RWTS [6].

### 3.5. Electrical power supply

The TSA-EPS receives AC power from the EPS (SBP-EPS), one of the plant systems, and distributes it to all the TS. It

also provides monitoring, control and protection of electric power distribution within its scope and provides on/off control of electrical power flow to the loads as well as the earthing equipment to all the TS.

The TC has an installed power of 2 kW, the HFTM, 154 kW; The STUMM, 33 kW, TSA, 2812 kW and the FCE, 60 kW. It is important to note that the major consumer is the TSA without counting the consumption of the helium double compressors, which are fed directly from the EPS mid voltage supply, each double compressor consuming up to 568 kW.

The TSA-EPS is comprised of 16 LV panels which provide power according to different types of supplies depending on the criticality of the customers. Six of them supply the non-SIC (Safety Important Components) electrical consumers, there are another six for SIC-2 components and four for SIC-1 components. In the case of the SIC-2 and SIC-1 panels, there are two of each, providing the electrical supply from two independent paths, making them redundant. All of them are subsequently classified depending on their voltage and whether they are uninterruptible or not. The ones uninterruptible are fed from the safety power subsystem that includes back-up diesel generators.

#### 4. The FCEs

Apart from the materials validation and other fusion-related activities for future fusion reactors, other experiments with a wide range of applications are envisaged at IFMIF-DONES [2]. There are two spaces foreseen in the facility for such applications: the room R160, downstream (figure 22) from the TC, and the room R026, below the AV (figure 23). The first one will take advantage from the continuous neutron stream from the TC, while the second one will use 1/1000 of the D+ beam being extracted and driven downwards by means of a kicker, an electrostatic septum, a magnetostatic septum, few quadrupoles and few dipoles.

##### 4.1. Room (R160) downstream from the TC

Room R160 has an area of approximately 300 m<sup>2</sup> and will include a few important components to enable the execution of dedicated experiments. The use of this room is yet to be defined by a proper experimental program, which, in addition, will lead to the definition of the hands-on maintenance and installation tasks and the installation of the experimental setups.

The neutrons present at the back of the TC will be transported via a 150 mm inner diameter duct, which is composed by two permanent sections, one inside the RBSB#11 and another one inside the bucket concrete downstream- and a set of rotating biological shielding barriers. The permanent sections compose the NBT while the rotating shielding wheels are included in an active mechanical device called NBS.

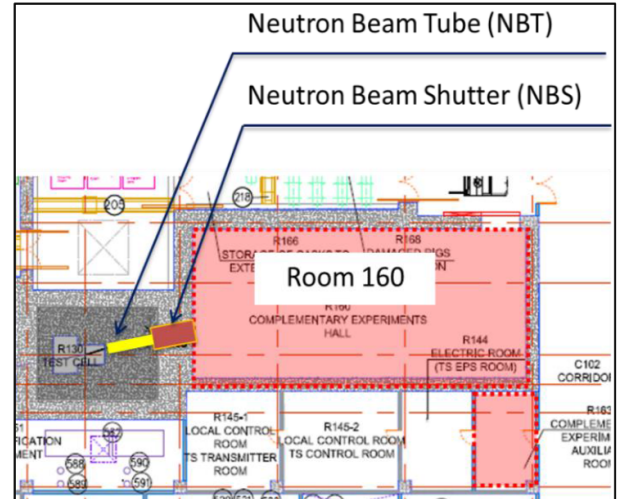


**Figure 22.** FCE room (R160) and its auxiliary room. The location of the NBT and NBS is shown as well.

The classification of this room is dual: yellow (maximal dose rate of 1 mSv h<sup>-1</sup>), for maintenance and installation of new setups, when the NBS is closed; red (forbidden access) when the NBS is open and experiments are running (beam on). In addition, that room must provide enough shielding to keep consistent dose rates in the adjacent areas according to the safety classification, e.g. green area (below 10 μSv h<sup>-1</sup>) in the corridor east side of the room. The layout of the shielding solution to do so is still under study.

With respect to the NBS, the figure 24 shows the shielding performance currently achieved according to the latest neutronics models. Further improvement, e.g. small local shielding pieces, is ongoing to avoid the very local neutron streaming slightly above 1 mSv h<sup>-1</sup> found at two horizontal cuts: at the level of the NBS driving shaft (figure 24 (top)) and the level of the NBT (figure 24 (bottom)), the latter via the NBS chart guides.

The NBS consists of two coaxial sections, each of them including rotating shielding discs (figures 25 and 26). The inner one has four short discs connected by pins and slots while the outer one has a big heavy shielding disc. The latter is planned to be used as a neutron filter and will have a set of five holes parallel to the shaft used as collimators/splitters for the neutron stream and where the moderators could be placed in. Both shielding sections can be controlled independently by their motors, which are located aside to minimize their interaction with the neutron fields coming from the TC. Such a way, the failure rate of those elements is reduced. In order to make the handling tasks in room R160 more manageable, the NBS is designed in a highly modular way, so the heaviest component is the disk #5, which weighs around 6 tons.

In case of accidental power blackout, the disks of revolving mechanism will autonomously (gravitationally) rotate back to closed position. This closure should occur in a relatively short



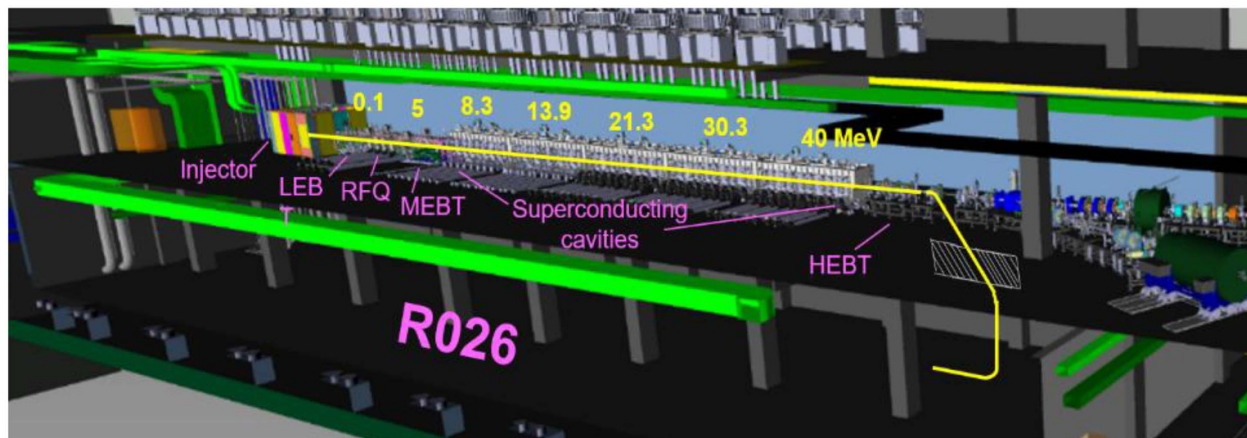


**Figure 23.** General 3D layout of the accelerator in the AV and the R026 below. Beam extraction towards R026 is symbolically shown as well.

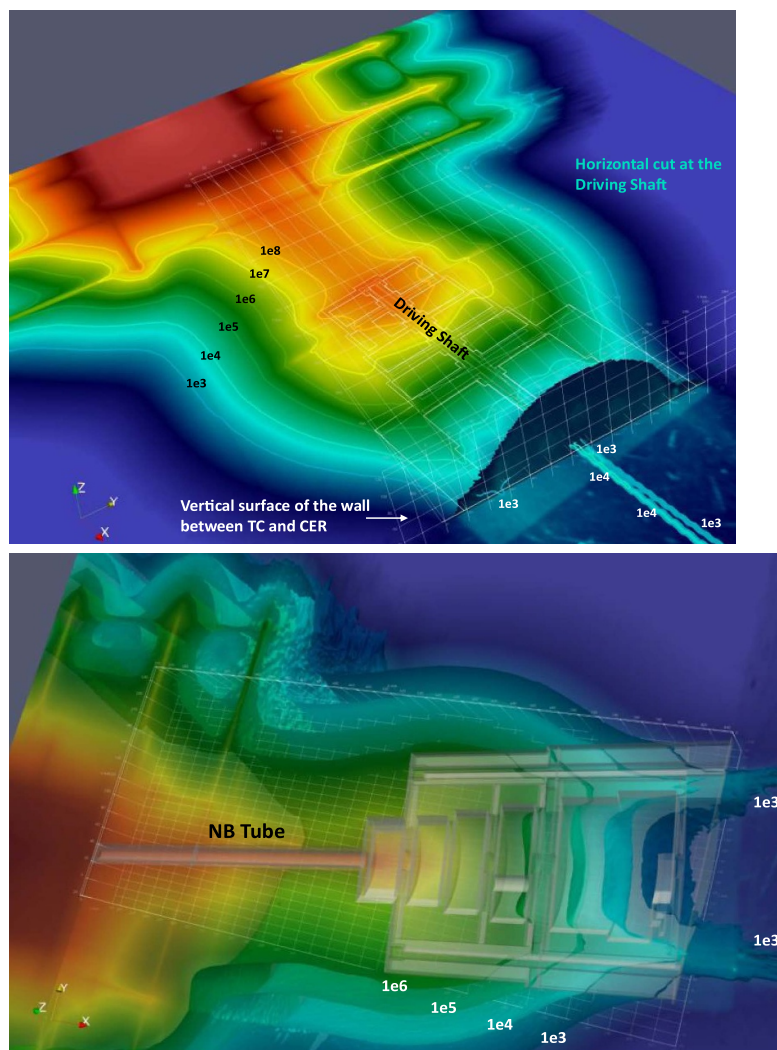


**Figure 24.** Top: horizontal cut of the dose rate (microSv/h) distribution map at the level of the NBS driving shaft. Bottom: horizontal cut of the dose rate (microSv/h) distribution map at the level of the NBT.

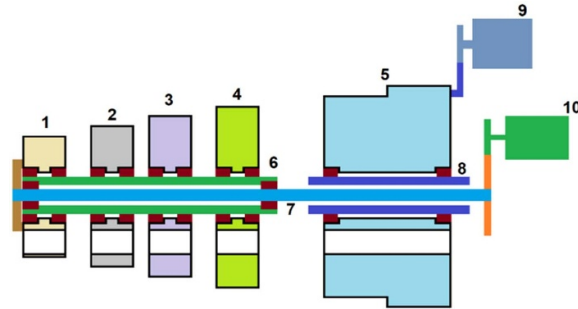


**Figure 25.** Representation of the disc arrays. 1: Disc #1; 2: Disc #2; 3: Disc #3; 4: Disc #4; 5: filter disc; 6: hollow shaft discs array; 7: internal shaft; 8: hollow shaft filter disc; 9: driving motor filter disc; 10: driving motor disc array.

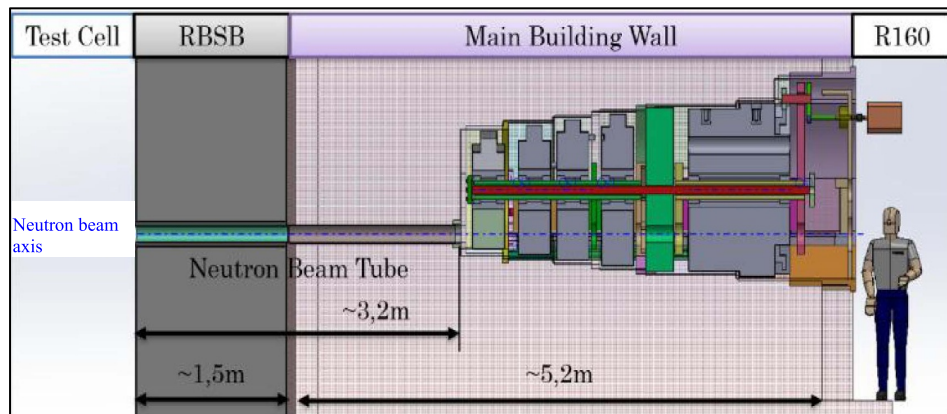


**Figure 26.** Overview of the NBS and NBT integrated in MB and TC.

transition period providing a passive safety function for room R160.

Room R160 will also include the necessary installation and maintenance tooling, and mediums (gases, vacuum, etc) required for the execution of scientific experiments.

#### 4.2. Pulsed beam facility (R026)

This facility will be placed in room R026, which has a ground area of 2871 m<sup>2</sup> with an average height of 7.4 m (with a total of 21 240 m<sup>3</sup>), representing a substantial volume available for the development of complementary experiments. This room allows for the inclusion of pulsed beam techniques, which is not possible in the other reserved spaces where only the use of a continuous neutron stream is permitted.

Apart from experiments using directly the pulsed deuterons, the production of pulsed neutrons with a maximum flux of  $7.4 \cdot 10^6$  n cm<sup>-2</sup> s is envisaged using a graphite/graphene target under vacuum conditions followed by several moderators to tailor the energy spectrum. Time-of-Flight (n-ToF) techniques will be used to determine the individual particle energies based on their path and velocity, and thus allowing a very broad range of reactions and experiments to be developed in this facility.

Furthermore, to enable these experiments, specific aforementioned devices are necessary to extract the pulsed, 1/1000 beam from the CW D+ beam in the AV. Besides, neutron production targets and various detection systems (based on

semiconductors, scintillators, GFM spectrometers...) will be required. All this hardware imposes additional maintenance and safety assessment requirements that will be defined as long as the experimental program is created.

In addition, the advancement of these operations calls for the integration of a multitude of plant systems, including the RWTS for wastes management, the HVAC system for room ventilation, the SGS and the SWS for gas and water services, the FPS and safety control system (SCS) for accident prevention, detection and mitigation.

## 5. Safety considerations and propagation to the TSs components

The classifications of the SICs are well described in [21]. Briefly and from the TS standpoint, there are two main safety functions. On one side, the first safety confinement barrier function concerns. (a) the TC liner (penetrations included), (b) the TCCP, (c) the closest valves -and its control- to the TC liner providing isolation to the fluids serviced to the TC, and (d) the circuits sections between the isolating valves and the TC liner. So all these components are SIC-1. On the other side, the shielding safety function is covered by components which are SIC-2 because they must preserve the SIC-1 components undamaged under a seismic event SL-2. In addition, they contribute to the shielding function in normal operation, which confirms the SIC-2 condition.

### 5.1. Quality standards of the TC

The first safety confinement barrier is well described in [21], the present paper showing its definition around the area of the TC (figure 4).

With respect to the TC liner, due to its size, it will be manufactured in various pieces that will be welded to each other to compose the whole component's main body. All those leak-tight weld beads will belong to the first safety confinement barrier, so they must be safety qualified and accepted by the Spanish Nuclear Council.

Besides this strong safety constraint, the top-level requirement in terms of availability of the plant is also a key point in the quality guidelines to be followed for the TC liner. Indeed, although the current concept of the TC allows for maintainability, a major failure in either the TC liner or one of the RBSBs would lead to a very long shutdown of the facility, in the order of 1 year or even longer.

This means that the quality standards to be applied to the TC liner need to be the highest ones whenever they balance well with the cost of component. This is an exercise currently ongoing although some tentative guidelines are being defined in the following terms:

- Raw material certificates with chemical composition (EN10204 Type 3.1).
- Buttwelding joints strongly preferred.
- Certificate 3.1 (EN10204) for the filled material: mechanical testing (tensile, Charpy), chemical composition analyses.
- Production of coupons of the buttwelding procedures involved.
  - Visual tests and penetrant tests for the bevels of the parts to be welded and the different steps of the coupon production: after tack welding, after root pass, complete coupon...
  - Mechanical testing: Charpy, tensile, bending...
  - Micrography.
  - Analyses for retained carbon content.
  - Chemical analyses.
- Qualification of the welders according to ISO 9606.
- Qualification of the workshops according to ISO 3834–2.
- Non-destructive analyses of 100% length of the bevels before welding.
  - Visual and penetrant tests.
  - Dimensional control of the parts (bevels) before welding.
- Non-destructive analyses of 100% of the weld beads length after welding.
  - Visual and penetrant tests.
  - Dimensional control of the parts (bevels) before welding.
  - Radiography test.
- Qualification of the personnel in charge of the tests.

Regarding the TC liner penetrations, seamless options have been considered in order to enhance their reliability this meaning that there are no weld beads upon the entire penetration. This is the reason why the cylindrical shape has been preferred. As a consequence, in the case of the penetrations sleeving

the TWBDs, neutron streaming will be minimized by proper shielding components inside the penetration and making the shape adaption inwards to the TWBD rectangular pipes.

The seamless option for cooling pipes for the water cooling circuits is likewise preferred, if possible. Otherwise, the main driver would consist of minimizing weldings on the pressure boundary and locating those in regions with the lowest neutron fluxes.

All these quality standards will keep the TC liner failure rate as low as possible within a reasonable cost of the component. Apart from this very high quality at the manufacturing phase of the component, regular *in-situ* maintenance actions could be also considered whenever they do not handicap so much the availability of the plant since they shall be implemented by RH techniques due to the very high residual doses inside the TC liner, which will discard any hands-on intervention.

On this regard, an option that could be applied with low impact on the plant's availability may consist of coupons cleverly located on the inner surfaces of the lower section of the TC liner, mainly next to the most critical weld beads. They should be easily inserted and extracted by RH means. After each or several irradiation campaigns, the coupons would be recovered for activation measurement and eventual post-irradiation testing that may include mechanical tests, micrography and other tests. This would be a way to monitor the degradation of the mechanical properties of the nearby weld beads. Quite importantly, those coupons will also give information about the helium content produced in the critical weld beads and its potential re-weldability in case of failure.

Together with the coupons, active *in-situ* inspection techniques would also add a further level of monitoring about the state of the TC liner. This *in-situ* inspection should be done by RH means and be implemented only from the inside because the outer side keeps inaccessible due to the RBSBs. With such access constraints, a promising inspection method, currently under exploration, may be based on eddy-current techniques since they can provide penetration depths as high as 19 mm for stainless steel AISI316L, which is consistent with the weld bead thicknesses currently present in the baseline design [22].

Concerning the stainless-steel raw material for the manufacturing of the vacuum vessel (TCCP and TC liner), the cobalt content will be controlled to ensure it is under a certain content, which is still to be defined although it must be balanced with the cost of such a huge vessel. Indeed, the lower the Co content the better to limit the activation of the material under the neutron fields inside the TC liner. On this regard, the cobalt activation is higher when subjected to thermal neutrons, which is the case at the location of the walls of the TC liner, away from the high irradiation region. Nevertheless, keeping a very low cobalt content may increase dramatically the cost of the vessel, so a preliminary target to be confirmed in this regard might be 1000 ppm of Co content. From the quality assurance point of view, material certificates with chemical composition will be mandatory.

The interfaces of the TC liner penetrations enclosing the TWBDs with the TIR liner belong to the 1st safety confinement barrier, so those leaktight welding beads must follow the



same quality guidelines as mentioned before. The same happens with the TC liner penetrations enclosing the IPA and OPA plugs.

Quite importantly, the accelerator beamlines cannot be safety-credited [21] due to the very high quantity of components and their complexity. This means that the welding beads between the TC liner penetrations and the TWBDs, which take part of the accelerator beam lines, are not safety credited, its main purpose being the leaktight volume and atmosphere segregation because the TIR volume will be filled with a slight-depression, argon-based atmosphere while the TC liner will be under a helium-based, rough vacuum of 90 mbar. The same happens with the interfaces between the TC liner penetrations and the outer surfaces of the IPA and OPA plugs, its main purpose being the volume and atmosphere segregation with respect to the LLC.

For those welding beads with leaktight volume segregation requirements only, a tradeoff will be carried out in order to provide the best quality as a good compromise in terms of cost. Indeed, the TC liner is still highly constraint by the availability requirement, so high-quality standards will be, anyway, required for these weld beads because a significant leakage in the vacuum vessel would lead to a dramatic, extremely long shutdown of the plant.

As mentioned before, the TC liner will be composed of several pieces welded to each other, trying to locate those weld beads as far as possible from the maximal neutron fluxes. Of course, this is somehow constraint by the maximal available sizes of stainless-steel plates of the required thicknesses and the limitation in terms of part size admissible by the mechanical manufacturing tools. Such an approach will lead to the minimization of helium production in the material due to the neutron fields, the maximal value being 1 appm He to ensure the feasibility of eventual re-welding. On this regard, for the most exposed weld beads to the neutron fields some local shielding could be considered, if necessary. Figure 27 shows the yearly He production on a vertical cut (XZ plane) of the TC liner.

Another strong safety guideline to be followed in the TC concerns the safety-credited hardware inside the TC liner. In principle, due to the extreme irradiation conditions inside, no component in the TC liner is being assigned any safety credit because it might not be possible to get qualified components under those unexperienced irradiation fields. Therefore, all the hardware inside the TC liner will not have any safety function, only monitoring purposes so, in case they fail no major consequence is expected in terms of the safety. As a result, the safety-credited hardware to keep the safety functions of the TS, e.g. isolation valves for the 1st confinement safety barrier must be included in the TSA, outside the TC. Further description in this regard can be found in section 5.2.

Some of the strongest drivers for the plant's systems design coming from safety lie on the so-called RASs. These scenarios have to be mandatorily considered on the design basis of the systems so they keep the safety functions even in those incidental cases. The TC liner is mainly a passive component such that its thermos-structural behavior copes with all the

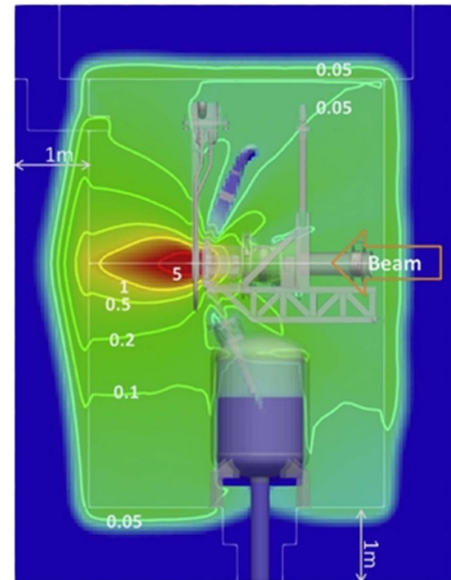


**Figure 27.** Vertical section of the He production map inside the TC liner (appm He/fpy) where 'fpy' means full-power year. Reprinted from [23], Copyright (2019), with permission from Elsevier.

RAS applicable. As mentioned above, the active components to keep the safety functions of the TC will belong to the TSA.

However, the convolution of all the RAS applicable has led to including the following asset in the vacuum vessel (TC liner and TCCP) design: the location of a rupture disk or safety release valve to mitigate an eventual sudden gas inrush through the accelerator beamline since the TAA or the TWBDs are not safety-credited components. At present, there is no DBA providing a pressure increase over the atmospheric pressure. Anyway, the uppermost part of the vacuum vessel will be provided with additional ports to enable the assembly of a rupture disk or safety release valve as shown in figure 9.

Finally, the only safety-credited, redundant diagnostic needed in the TC concerns the pressure transmitters monitoring the pressure inside the volume of the upper section.

## 5.2. Safety drivers to the TSA

The definition of the quality standards to be applied to the different TSA subsystems is pending. Nevertheless, they will take advantage of other facilities -or even industrial plants- with similar systems. Therefore, this section is focused on a few specific drivers coming from the particularities owned by IFMIF-DONES as one-of-a-kind facility worldwide.

Due to the current definition of the first safety barrier confinement, all the active safety-credited elements to provide isolation to the TC liner must be outside the TC and exposed to dose rates low enough to not compromise their performance. Therefore, those active elements must be either in the AC or in the TSA room (yet to be defined). In addition, they will belong to the different loops or circuits that provide penetrations in the TC liner via the feedthroughs placed in its upper section, which, in turn, leads to each of those TSA subsystem -HCS-LP/MP and GPS- to include two redundant

normally-closed isolation valves as close as possible to the feedthroughs (figure 21). In addition, all these short branches from the feedthroughs to the isolation valves will also include safety-credited redundant pressure transmitters and, only in the case of the GPS, safety-credited redundant flowmeter. In the case of the WCS, since the water cooling can be a mitigation capacity in incidental events, just the flow meters close to the inlet and outlet of the RBSBs and the TC liner will require safety credit and redundancy.

Apart from the considerations related to the first safety confinement barrier, the WCS may also be concerned by the need of a decay volume, which final location is still pending. Anyway, the arrangement of the WCS hardware in the TSA room already has a space reservation for an eventual decay volume.

Eventually, the different loops of the TSA have already more conventional, but safety-related, devices like safety relief valves and guard vessels to avoid excessive overpressure in the circuits.

### 5.3. Safety drivers to the FCE

Concerning the shielding function, the only active component involved is the NBS, which means that it has to provide safety-credited signal about the position of the shutter.

In a wider sense, although not detailed in this article, the rooms for the FCE will have specific radio-protection and safe-access requirements for workers or personnel that should go in. This will be managed by the corresponding access and radio-protection mandatory procedures defined by the Safety Department of the facility. The access to the rooms will be also managed by the PASS integrated in the SCS.

### 5.4. Safety drivers to the TS LICS

For each system, there will be a LICS in charge of its control. Each system with safety-credited devices or diagnostics will integrate a specific segregation devoted to the SCS in its LICS. All the safety-related signals will be managed and transmitted under highly reliable, timely routes from the safety-credited hardware to the LICS cubicle. The TS system most concerned by this guideline is, by far, the TSA. The FCE is up to some extent, also affected, as well as the TC, although very slightly.

## 6. Alignment strategy inside the TC

The present section describes the alignment strategy currently applicable to IFMIF-DONES according to the present baseline. Further stages towards a final design of the plant will include tasks like a plan for the integration of alignment activities in between the erection of the MB and a complete error and uncertainties budget and its translation to the final design of the components by means of appropriate mechanical tolerances.

### 6.1. General introductory notions

There are two key elements of the facility installed inside the TC, the TAA and the HFTM. Both must be aligned with the beamline of deuterons produced by the accelerator system.

The biggest challenges for the alignment in the IFMIF DONES facility are: (1) the systems to be aligned with respect to the global coordinates system are installed in different rooms (figure 28), (2) some elements (e.g. TAA and HFTM) are in a very radioactive area which prevents manual handling. The fact that no manual handling is allowed for alignment implies that a hard-rad fiducial needs to be continuously installed with each equipment that becomes radioactive and the adjustments in position must be done via RH.

The reference points fixed on walls and floor for the alignment will be named in this article CPs, but in the literature are also known as monuments or nests. There is a network of CP in the AV, where most of the main accelerator systems are installed, and a laser tracker will be used for the alignment of such elements. Part of the strategy and the instrumentation defined for the alignment at IFMIF DONES is related closely to the one from the LIPAc accelerator [24, 25]. There is also a network of CP in the walls and floor of the AC, which is the room from which sight lines to the key systems inside the TIR and the TC are enabled whenever the corresponding shielding plugs are removed.

In order to align, in the same global coordinates system, all the key systems of the accelerator in the AV and the TIR, as well as the TAA and the HFTM in the TC, the AV CPs network and the AC CPs network need first to be properly linked.

This is enabled by means of three holes (figure 29) that are closed with cylindrical shieldings during normal operation. In addition, the cylindrical shieldings are covered with a blind flange avoiding air passing between the two rooms (figure 29). The need to connect the two CPs networks and calibrate positions periodically is fully justified by the differential settlements of this huge concrete structures as illustrated in [26], where displacements in the order of 3 mm were measured. The use of holes temporarily open for the connection of CPs network was used successfully by INFN as illustrated in [27]. The detailed procedure and uncertainty results applied to IFMIF DONES is described in [28], the present article providing further progress and update w.r.t the latter.

### 6.2. Fiducials and adjustable elements for TAA and HFTM

The TAA will be subjected to extremely hard irradiation fields so, at present, a yearly 20 days maintenance period is foreseen to replace it by a new one. In addition, the removal of the TAA implies the previous removal of the HFTM, which may also need replacement or not depending on the IFMIF-DONES irradiation programme and the state of degradation of the module. Upon each insertion of those key elements, a position check is advisable, a remotely managed laser radar located in the AC (figure 29) will be used to look at the corresponding fiducials.

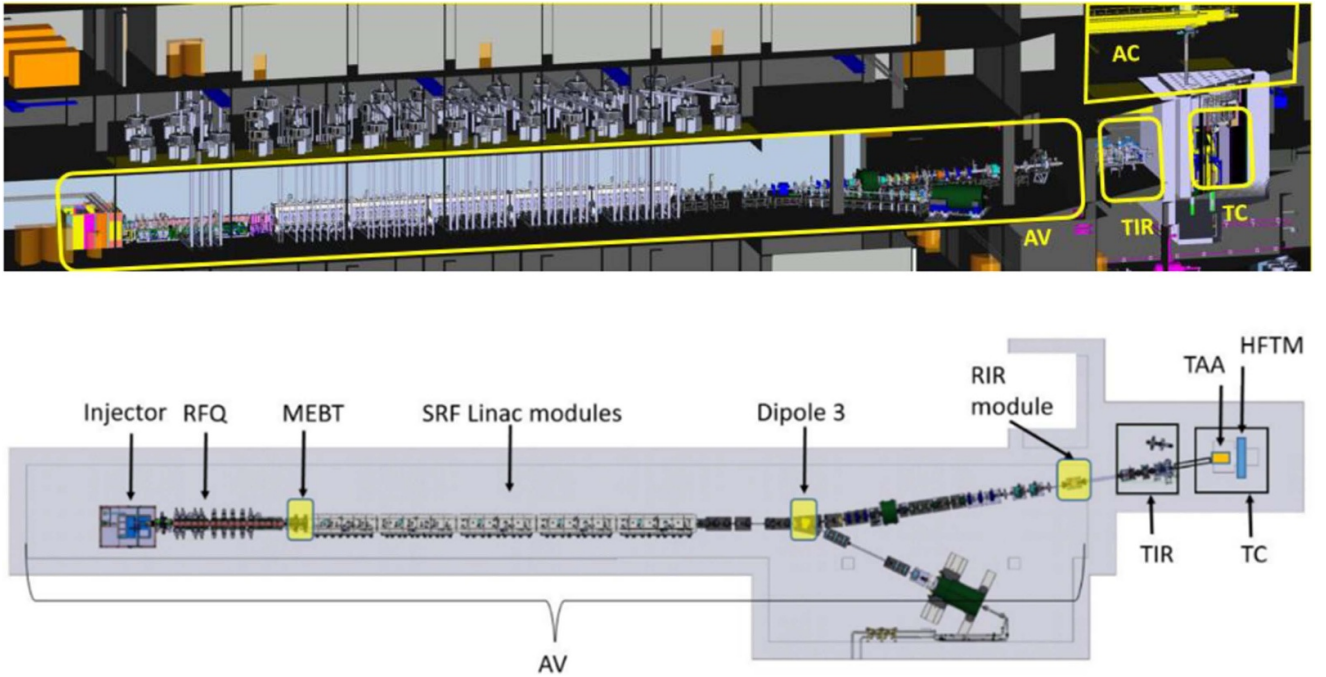


**Figure 28.** Top: general view of the rooms housing key systems to be aligned w.r.t the global coordinate system (GCS). The AC does not house any key system to be aligned but it has a key role to enable the leap frogs required to link the positions of the AV equipment and TIR equipment with the GCS, which is located inside the TC. Bottom: top view of the layout of the equipment to be aligned and its distribution in several rooms: accelerator systems in the AV and the TIR; TAA and HFTM in the TC.

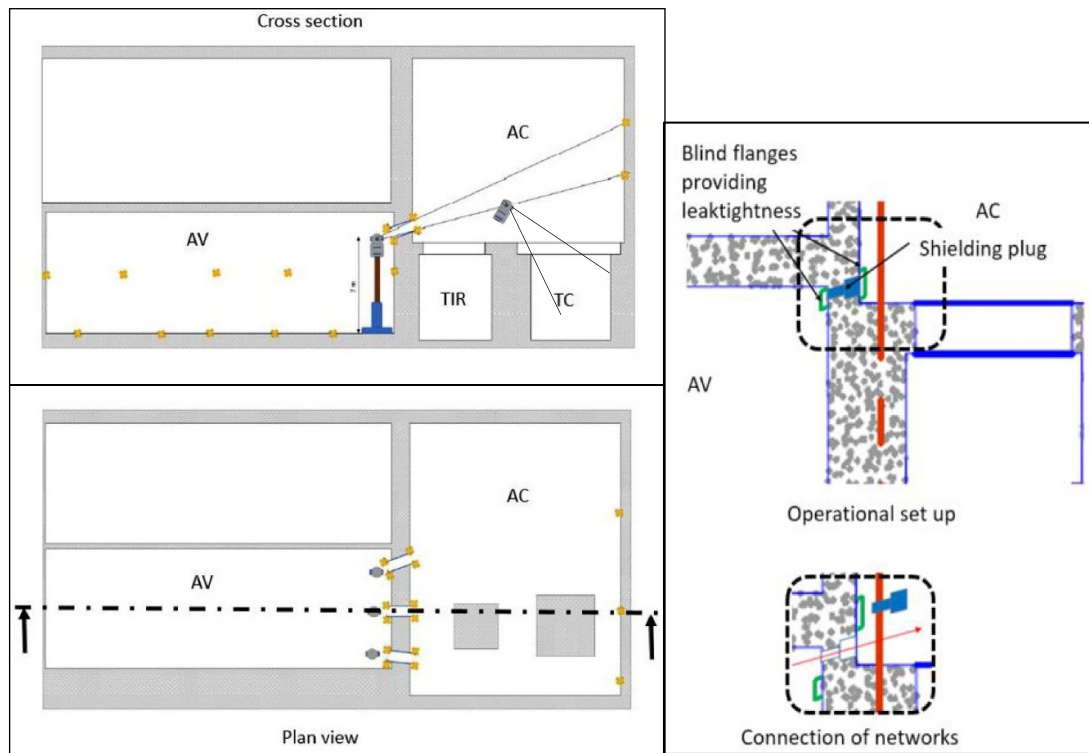


**Figure 29.** Left: top view (bottom) and cross section (top) sketches of the holes for leapfrogging between the AV CP and the AC CP networks. Right: detailed sketch showing the isolation between the AV and the AC by the shielding plugs, which are made of cylindrical concrete with a labyrinth shape (operational setup). The blind flanges and the shielding plugs are removed during the connection of AV CP and AC CP networks.



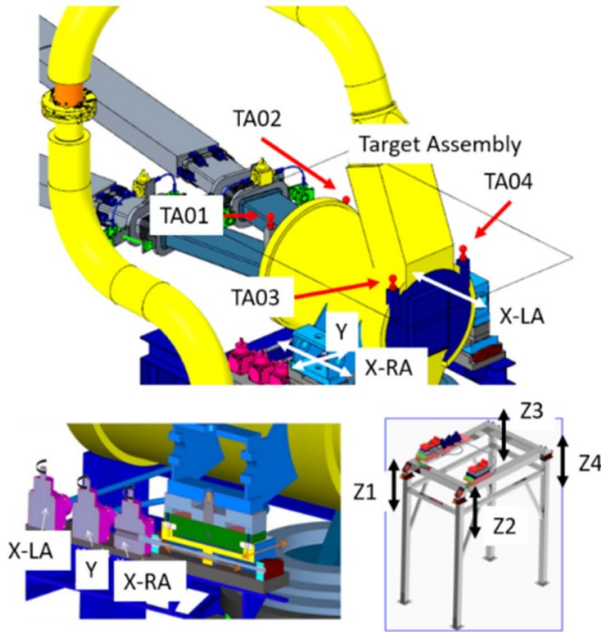


**Figure 30.** Top: target assembly with the fiducials TA01 to TA04. Bottom left: adjusting mechanisms for horizontal displacements and vertical rotation. Bottom right: joints for vertical displacement and horizontal rotations.

The fiducials in the TAA (TA01 to TA04) (figure 30) are stainless steel spheres that remain in place during irradiation. Due to high radiation doses, no manual use of Spherically Mounted Retroreflectors is allowed, and they cannot be left installed because radiation and high temperatures would distort their reflection properties. Instead, the stainless-steel spheres are radiation resistant but require the use of a laser radar that scans part of the surface and computes the coordinates of the system.

Those spheres may become rusty with the irradiation, but the laser radar is still capable of capturing its center and location.

The maximal XY error position defined for the D+ beam w.r.t the TAA and the HFTM is  $\pm 10$  mm, which has been split into  $\pm 5$  mm for the D+ beam XY position with respect to the GCS, and  $\pm 5$  mm for the HFTM and TAA XY position with respect to the GCS. This error budget prevents, as a quite conservative approach, from a catastrophic hitting of the D+ beam against unwanted surfaces of the beamline. Therefore, some positioning tuning mechanisms have been foreseen and included in the current baseline, such that the HFTM can be tuned within a range of 40 mm in X and  $\pm 10$  mm in Y, while the TAA can be tuned within a range of  $\pm 10$  mm in X and  $\pm 5$  mm in Y.

The support structure of the TAA includes three flexible axis that provide degrees of freedom in X-LA (left axis), X-RA (right axis) and Y axis. The six degrees of freedom of the solid body are achieved with axial joints, one per leg of the structure, being therefore one redundant. Successive stages of measuring of fiducials and implementation of correction of position with a robotic arm actuating in each of the joints would eventually get the TAA in the desired ‘installation position’.

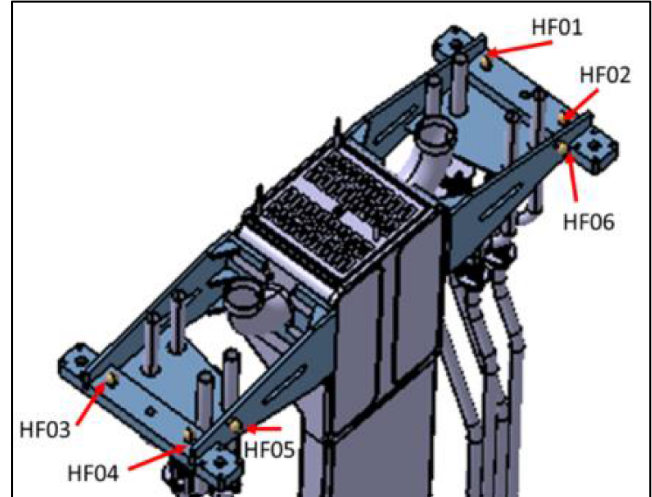


**Figure 31.** High flux test module showing the position of the six fiducials and the local coordinates system.

The position of the HFTM is determined by six fiducials (HF01 to HF06) as seen in the figure 31. These fiducials are located at the top of the equipment in order to facilitate the localization with the laser radar. Their coordinates are first measured with respect to the local coordinates system, which is placed in the middle of the area hosting the test specimens to be irradiated. This measurement is done when the equipment is not yet irradiated in a metrology laboratory. Subsequently, the coordinates of the fiducials are transferred to the global coordinates system by applying the corresponding translations and rotations. Finally, the correct positioning of the fiducials during the alignment process, will lead to the right ‘installation position’ of the test specimens receiving the neutron flux.

The degrees of freedom in the alignment process of the HFTM are governed by the following devices shown in figure 32: (1) two eccentric bolts providing independent translation in the X axis (TX), (2) one eccentric bolt providing translation in the Y axis (TY), (3) two vertical bolts providing translation in the vertical axis, (4) two connections (C-A, and C-B) fixing the distance with respect to the TAA.

One of the key relative distances to achieve with very low uncertainty is the distance between the rear outer surface of the TAA, and the front surface of the HFTM. This distance must have a nominal value of 2 mm, with as low deviation as possible, even when heterogeneous temperatures distributions deform the structures. This is the reason why the connections C-A and C-B keep a physical link preventing the two elements move away, distorting the neutrons flux received in the specimens, or move closer to each other risking a potential clash and the resulting damage.

### 6.3. Shifts from alignment to working conditions

The installation and alignment of the TAA and the HFTM will be done at room temperature and atmospheric pressure. Nevertheless, during operation, the liquid lithium will be flowing at 300 °C inside the pipes and the TAA. In addition, the

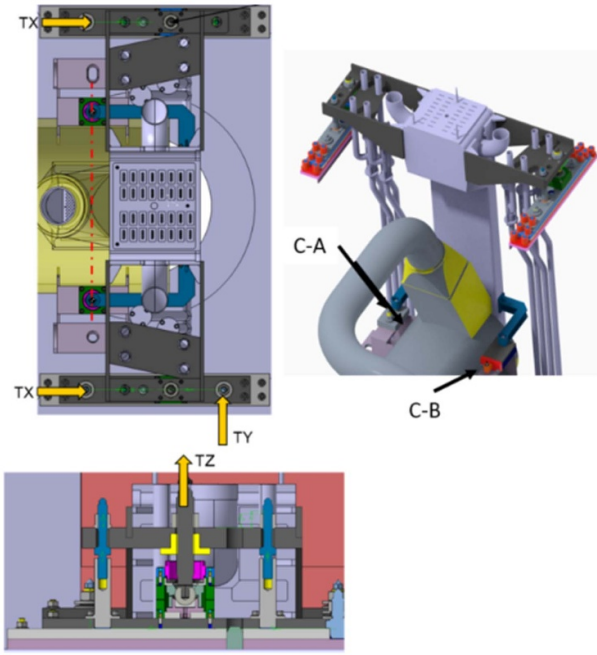


**Figure 32.** Top left: translations with eccentric bolts in the horizontal plane. Bottom left: vertical translation with two bolts (one per side, only one seen in the picture). Right: view showing the physical connections of the HFTM with the TAA.

whole TC liner will have been vacuumed just to keep residual helium at 90 mbar in operation, the nuclear heating produced by the neutron fields affecting all the in-vessel components and systems, even if cooled down by helium gas as in the case of the HFTM. The TC liner walls -mainly in the low section- will also present a thermal distribution as a result of the steady state between the nuclear heating and the water cooling on its outer surfaces.

On one hand, as explained in section 2.2.3.3, the TC liner baseline limits the shifts -from alignment to working conditions- induced in the key in-vessel components and systems to around 2 mm in the worst case. On top of this, thermal shifts are expected on the TAA inside the TC liner. The changes in position that are more relevant for the core process of the stripping reaction generating neutrons are those in the backplate of the TAA, which are around 1.2 mm in  $X$  direction (figure 33) and 2 mm in  $Z$  direction, the displacements along  $Y$  being negligible.

During the installation and alignment of the in-vessel components, these shifts will be considered beforehand so for each of them the following positions are defined:

- ‘Nominal position during irradiation’: theoretical position of the center of the local coordinates systems of the in-vessel system or component -TAA and HFTM- at working conditions, assuming that the beam is at its nominal position as well.
- ‘Installation position 01—IP01’: position of the center of the local coordinates systems of the in-vessel system or component -TAA and HFTM- wanted at the end of the alignment

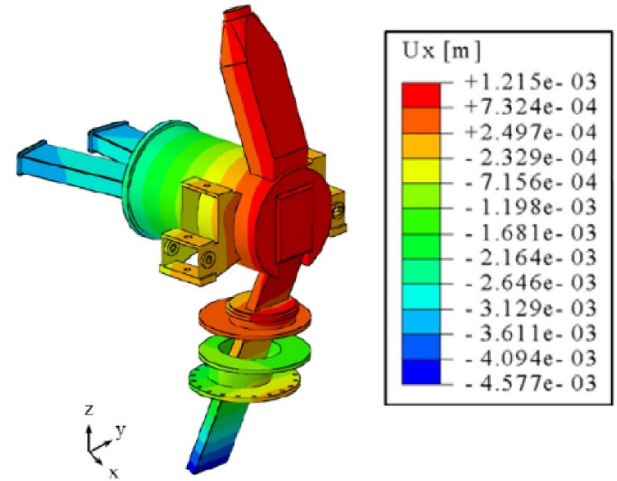


**Figure 33.** Displacements along  $X$  of the TAA due to thermal loads during operation.

(TC open, room temperature), compensating the deformations that will take place later on when the machine will be carried to working conditions.

Finite element method calculations provide the displacements that we have to deduce for the determination of IP01. It is also planned to use a range of electric heaters in a mock up TAA and HFTM to physically reproduce the temperatures distribution before even the first irradiation is initiated. This activity will be part of the commissioning (section 7). The measured values would provide a realistic approach to the expected displacements and will allow for benchmarking of the thermal-structural models of the TC liner and the in-vessel systems.

## 7. Notions about the integrated commissioning inside the TC

The commissioning of the facility will be implemented according to a staggered approach [29] starting with the accelerator, that will take three phases by itself up to its beam dump. The last section of the accelerator will be commissioned during the fourth phase, together with the lithium target and the STUMM. Of course, to reach this point in good shape, the TC will have successfully fulfilled its own testing phase, as well as the TSY. This means that, at this moment, basically all the plant systems and all the ancillary systems are ready.

The first time a beam hits the lithium target, the STUMM will also be there. The main objective of the latter consists of providing the benchmarking of the theoretical models about the irradiation fields inside the TC liner, mainly in its high-flux region. After the commissioning, once the models have been consistently benchmarked, the prediction about the irradiation models applicable to the high-flux region with the HFTM will be much more precise.

Some first notions have been already defined about the different stages of phase IV of the commissioning:

### 7.1. Starting up and detecting the beam

The objective of this stage is to get a first beam hitting the lithium target safely. Therefore, the beam will be displayed at quite low power and in pulsed mode to protect the machine, i.e. the accelerator hardware and beamline walls, in case of very significant shift w.r.t its nominal position. Moreover, the beam size will be significantly small w.r.t the nominal range of sizes.

As an output for this stage, the beam position and size on the target should be well captured by means of the proper diagnostics in the HEBT system, the lithium diagnostics and the STUMM diagnostics. Quite importantly, the TC liner walls will also be populated with a certain number of detectors, micro-fission chambers, ionization chambers, gamma thermometers and SPNDs- cleverly placed to provide information about the state of the irradiation fields in the TC liner. From this stage onwards, relationships between the diagnostics on the TC liner and the diagnostics in the STUMM will try to be found through data processing. If this may be confirmed during the commissioning, the TC liner diagnostics may play an important role in monitoring the state and position of the beam during the steady state of the machine, which might allow for a low quantity of detectors in the HFTM, thus maximal volume available for payload being provided. In addition, as the TC liner walls are irradiated with fluxes orders of magnitude lower than in the high-flux region, the reliability of those diagnostics would be higher.

Eventually, the positions of the in-vessel systems at this point will be so-called ‘Installation Position IP01’ (section 6.3). If necessary, some slight steering of the beam from the Accelerator Systems may be required.

Due to the low duty cycle of the beam, nuclear heating is expected to be much lower than in CW conditions. This means that, at the end of this stage, the in-vessel systems will still not be in its ‘Nominal position during irradiation’ (section 6.3). Anyway, the cooling systems of both the lithium systems and the TSs will start working and dissipate the heat produced.

### 7.2. Centering and enlarging the neutron footprint

The objective of this stage is to increase the duty cycle of the beam and its size, so the irradiation conditions are converging towards the final steady-state at CW.

Continuous monitoring of the beam size and position will be implemented while the frequency of the pulses is increased step by step. At each step, higher nuclear heating will be provided to the in-vessel systems, so real time feedback will be necessary to keep the beam safely in the central zone of the target. The beam size will also be gradually enlarged to get closer to the  $10 \times 5 \text{ cm}^2$  size.

As the deposited energy will increase much during this stage, relative shifts are expected of the beam w.r.t the in-vessel systems. In fact, shifts will come from the displacements of the in-vessel systems due to its very significant

increase in temperature, as well as from the accelerator due to the increase of power of some of its systems to cope with the higher duty cycle.

As an output from this stage, the beam characteristics should be quite close to the CW, steady-state condition and its position should be, with certain error margin, well centered onto the lithium target. The in-vessel systems will be close to its thermos-structural steady-state, the lithium flow taking a very high power, i.e. almost 5 MW, coming from the stripping reaction.

### 7.3. Reaching full-power CW steady-state and testing the range of beam sizes

The objective of this stage is to get the steady state of the machine with the beam placed on the nominal position during irradiation. Firstly, the beam size will be the smallest from the nominal range of sizes:  $10 \times 5 \text{ cm}^2$ . Afterwards, the beam size will be, step by step, enlarged. At each step, the machine will require some time to get its new steady state, for which some beam tuning may be needed to place it in the nominal position.

During this stage the steady state conditions must be reached so relatively long time will be necessary for all the systems to get their thermal and thermo-structural steady states.

### 7.4. Benchmarking of the neutronic theoretical models

Once all the machine has reached the full power steady-state condition, data gathered from all the detectors of the STUMM will be compared to the theoretical data from the neutronic models. Most of all these data will be integrated values since most of the detectors gather integrated effects through all the range of energies produced by the stripping reaction. Nevertheless, several diagnostics based on activation specimens will be available in the STUMM in order to give the fluxes applicable to some specific energies.

As an output from this stage, the neutronic models should have been corrected according to the real performance of the machine under CW steady-state conditions. Those models should be ready to predict the signals for the HFTM and TC liner neutron diagnostics.

Therefore, the machine would be ready to replace the STUMM by the HFTM. Depending on the duration of the CW stage of commissioning, the TAA should also be replaced.

## 8. Conclusions

Through the present work a comprehensive overview of all the TSs at IFMIF-DONES has been given, except for the irradiation modules, which will have a specific article in this special issue.

The overview has been updated according to the status of all the engineering work currently ongoing. The transversal areas -safety, maintenance, logistics, quality assurance,...-



have been also included as per the scope of the TSs and their propagation in terms of requirements and design features.

Concerning the TC, the components have been described, their critical features being addressed regarding their performances against the most important requirements.

On this regard, shielding performance is currently in good shape although there are some local spots requiring further improvement of the design. From thermal point of view, the TC keeps in good shape as well since the average working temperature expected in the vacuum vessel is foreseen to be well below the requirement (50 °C–60 °C). Likewise, the RBSBs are kept, according to the present design, within a thermal safe range (around 95 °C in the worst case) to preserve properly the water content for the neutron shielding. Likewise, the current design has been also focused to enable a non-maintainable Bucket floor, thus the nuclear heating deposited there being minimized.

From structural point of view, the vacuum vessel has been also analyzed under the most severe load case, seismic plus operation loads, to ensure fulfillment as part of the first safety confinement barrier.

Very importantly, several quality guidelines have been also listed for the most critical components of the TC in order to maximize the availability and the safe operation of the plant. Safety requirements have been also propagated to other TSs, i.e. the TSA and the FCE.

Concerning the latter, critical components like the NBS have been explored from neutron analyses point of view to ensure the dual classification of the room R160 in beam-on conditions: yellow, if NBS is closed (restricted access for maintenance and installation); red, if NBS is open and experiments running in the room.

Last but not least, a description has been given about the main approaches for transversal activities like the alignment of the in-vessel components and the integrated commissioning in the TC.

Overall, this work provides the reader with a clear understanding of the updated status and complexity of these crucial systems in IFMIF-DONES, which are at the core of the plant, as well as a comprehensive overview of the design, stressing the aspects and features leading to the compliance with the most critical requirements. Consequently, one can infer that, although further work is, of course, needed, the current baseline is in good shape to ensure the main functionalities of the facility.

## Acknowledgments

This work has been carried out within the framework of the EUROfusion Consortium, funded by the European Union via the Euratom Research and Training Programme (Grant Agreement No. 101052200—EUROfusion). Views and opinions expressed are, however, those of the author(s) only and do not necessarily reflect those of the European Union or the European Commission. Neither the European Union nor the European Commission can be held responsible for them.

## ORCID iDs

S. Becerril  0000-0001-9009-1150  
 J. Castellanos  0000-0001-5637-3322  
 P. Araya  0009-0008-9413-0071  
 F. Arranz  0000-0002-9591-4096  
 R. Michalczuk  0000-0001-6499-3812  
 F. Mota  0000-0002-1337-2482  
 I. Podadera  0000-0002-3459-4631  
 M. Ruiz  0009-0005-9393-325X  
 A. Serikov  0000-0003-2053-7879  
 A. Zsákai  0000-0002-0645-3487  
 A. Ibarra  0000-0002-2420-2497

## References

- [1] Zsákai A. *et al* 2024—Evolution of IFMIF DONES' heart: system overview of the test cell *J. Nucl. Mat.* **598** 155185
- [2] Ibarra A., Królas W., Bernardi D., Cano-Ott D., Becerril-Jarque S., Álvarez I. and Qiu Y. (EUROfusion WPENS Team) 2025 DONES performances, experimental capabilities and perspectives *Nucl. Fusion* **65** 122006
- [3] Maestre J. *et al* 2025 Overview and current status of the IFMIF-DONES lithium systems *Nucl. Fusion* **65** 122011
- [4] Kondo K. *et al* 2014 Neutronic analysis for the IFMIF EVEDA reference test cell and test facility *Fus. Eng. Des.* **89** 1758–63
- [5] Arbeiter F. *et al* 2025 The IFMIF-DONES irradiation modules *Nucl. Fusion* **65** 125001
- [6] Luque M., Ruiz López M.F. and Ibarra Á. 2025 IFMIF-DONES buildings and plant services *Nucl. Fusion* **65** 122002
- [7] Oravecz D. *et al* 2024 Updates of the removable biological shielding blocks inside of the test cell, part of the test systems of IFMIF-DONES *Fusion Eng. Des.* **200** 114179
- [8] Kenjo S., Oyaidzu M., Obata K., Ochiai K. and Sato S. 2024 Assessment on liquid Li fire risk under humid air condition and with heat insulators *Nucl. Mater. Energy* **38** 101569
- [9] Ruiz López M.F., Maestre J., Beltran F., Torregrosa-Martin C., García M., García-Macías E., Gallego R. and Ibarra Á. 2025 Seismic safety strategy for IFMIF-DONES *Nucl. Fusion* **65** 122001
- [10] Hilsdorf H.K., Kropp J. and Koch H.J. 1978 The effects of nuclear radiation on the mechanical properties of concrete *ACI SP-55, Douglas McHenry Int. Symp. on Concrete and Concrete Structures* (American Concrete Institute)
- [11] Micciché G. *et al* 2025 Remote maintenance in IFMIF-DONES: current status and future development program *Nucl. Fusion* **65** 122007
- [12] Piotrowski T. *et al* 2024 Optimization and evaluation of structural and shielding concrete for IFMIF-DONES *Nucl. Mater. Energy* **38** 101597
- [13] Mazza F., Mazza M. and Vulcano A. 2017 Nonlinear response of r.c. framed buildings retrofitted by different base-isolation systems under horizontal and vertical components of near-fault earthquakes 테크노프레스 *Earthquakes Struct.* **12** 135–44
- [14] Ghiocel D.M., Kostarev V., Kultsep A. and Nawrotzki P. 2022 A study on seismic SSI analysis of a base-isolated storage structure founded on firm soil *Proc. 26th Int. Conf. on Structural Mechanics in Reactor Technology (Smirt-26) (Berlin/Postdam)* (available at: <https://www.proceedings.com/content/069/069112webtoc.pdf>)
- [15] RCC-MRx code- (available at: [www.afcen.com/en/106-rcc-mrx](http://www.afcen.com/en/106-rcc-mrx))

- [16] Ghojel J. 2002 Application of inverse analysis to thermal contact resistance between very rough non-conforming surfaces *Inverse Prob. Eng.* **10** 323–34
- [17] Ghojel J. 2004 Experimental and analytical technique for estimating interface thermal conductance in composite structural elements under simulated fire conditions *Exp. Therm Fluid Sci.* **28** 347–54
- [18] Espinos A., Romero M.L. and Hospitaler A. 2010 Advanced model for predicting the fire response of concrete filled tubular columns *J. Constructional Steel Res.* **66** 1030–46
- [19] Ding J. and Wang Y.C. 2008 Realistic modelling of thermal and structural behaviour of unprotected concrete filled tubular columns in fire *J. Constructional Steel Res.* **64** 1086–102
- [20] Tao Z. and Ghannam M. 2013 Heat transfer in concrete-filled carbon and stainless steel tubes exposed to fire *Fire Saf. J.* **61** 1–11
- [21] Torregrosa-Martín C., Martín-Fuertes F., Marugán J.C., Qiu Y. and Ibarra A. (the EUROfusion WPENS Team) 2025 Safety analysis and licensing approach of IFMIF-DONES *Nucl. Fusion* **65** 122009
- [22] Gelatko M., Hatala M., Botko F., Vandžura R. and Hajnyš J. 2022 Eddy current testing of artificial defects in 316L stainless steel samples made by additive manufacturing *Technol. Mater.* **15** 6783
- [23] Qiu Y., Arbeiter F., Fischer U. and Tian K. 2019 Neutronic analysis for the bio-shield and liners of the IFMIF-DONES test cell *Fusion Eng. Des.* **146** 723–7
- [24] Scantamburlo F. *et al* 2014 Alignment of LIPAc, the IFMIF prototype high current deuteron accelerator requirements and current status *Proc. Int. Workshop on Accelerator Alignment* (available at: [www.slac.stanford.edu/econf/C1410132/papers/126.pdf](http://www.slac.stanford.edu/econf/C1410132/papers/126.pdf))
- [25] Scantamburlo F. *et al* 2016 LIPAc, the IFMIF/EVEDA prototype accelerator: alignment and assembly current status and possible future improvements *Proc. Int. Workshop on Accelerator Alignment* (available at: [www.slac.stanford.edu/econf/C1610034/papers/832.pdf](http://www.slac.stanford.edu/econf/C1610034/papers/832.pdf))
- [26] LeCocq C. *et al* 2022 LCLS LCLS-II survey and alignment (SLAC Metrology Department) (available at: [www.slideserve.com/oriel/lcls-lcls-ii-survey-alignment](http://www.slideserve.com/oriel/lcls-lcls-ii-survey-alignment))
- [27] Pellegrino L. *et al* 2016 A technique for the transport of an alignment networks through a small hole *Proc. 14th Int. Workshop on Accelerator Alignment* (available at: <https://indico.cern.ch/event/489498/contributions/2217544/>)
- [28] Arranz F. *et al* 2024 Alignment strategy for IFMIF-DONES facility *Fusion Eng. Des.* **200** 114181
- [29] Podadera I. *et al* 2022 Commissioning Plan of the IFMIF-DONES Accelerator *31st Int. Linear Accelerator Conf. LINAC, TUPOJO* pp 330–3